RESEARCH ON THE FILTRATION OF COMPRESSIBLE CAKES

Final Report to the

Water Research Commission

by

VL Pillay

Pollution Research Group
Department of Chemical Engineering, University of Natal
Private Bag X10, Dalbridge 4014

WRC Report No 241/1/98

ISBN 1 86845 435 5

EXECUTIVE SUMMARY

RESEARCH ON THE FILTRATION OF COMPRESSIBLE CAKES

by

VL Pillay

1 BACKGROUND TO PROJECT

Filtration is widely employed in the water industry, for the clarification of suspensions, the concentration of suspensions and the dewatering of sludges. In most instances, the cakes formed are compressible, i.e. it undergoes changes to its structure and properties during the filtration process. This can significantly affect the performance of the filter, as well as introduce seemingly spurious system behaviours. Accordingly it is necessary for workers in the filtration field have a knowledge of the mechanisms that determine cake compression and the effects that compressible cakes have on systems.

The design and optimisation of filtration systems would be significantly improved if the performance of the filter under different operating conditions and configurations could be predicted. This would be possible if the compressibility characteristics of the cake could be quantified and employed in appropriate filtration equations. The prediction of filter performance from sludge characteristics would also greatly assist in determining the effectiveness of sludge conditioners and coagulant aids, prior to implementing them on an operating plant.

Various sludge characterisation tests have been reported in the literature. However, the only test that seemingly enjoys a degree of application is the Buchner Funnel test. Although this can be used to obtain an indication of the relative resistance of a cake, it is inadequate in reasonably predicting compressible cake properties and filter performance. Other tests, e.g. the compression-permeability test and the settling test, are not widely employed, possibly due to contradictory claims regarding their validity as well as a lack of knowledge of how to perform the tests. The basic filtration equations are also rarely employed in optimising filtration systems. This could be due to the perceived difficulty in obtaining basic CPV data.

The aim of this study is to acquaint workers in the water field with the effects associated with compressible cakes, and to identify and develop methodology that would enable workers to characterise compressible cakes and predict the performance of large scale filters from laboratory tests and the basic filtration equations.

2 OBJECTIVES

The objectives of this project are as follows :

(i) to investigate the mechanisms responsible for compressible cake behaviour,

(ii) to investigate the effects that compressible cakes have on filtration systems,

(iii) to investigate methods to characterise cake compressibility,

(iii) to identify and develop models and equations to predict filtration performance for compressible cake systems.

3 REALISATION OF OBJECTIVES

The mechanisms responsible for cake compression in filters have been investigated. The major cause of cake compression in filters is hydraulic compression, where fluid frictional forces cause particles to irreversibly infiltrate existing void spaces, leading to a more densely packed cake of reduced voidage and permeability. As a result of hydraulic compression, solids compressive pressure, permeability and voidage profiles are established through the cake. Further, the resistance of the cake layers to fracture by axial shear forces also varies along the thickness of the cake. A major feature of hydraulic compression is that it is irreversible, i.e. once a layer in a cake is exposed to a higher pressure it maintains the consolidation appropriate to that pressure even if the pressure is subsequently lowered.

This hydraulic compression of the cake has various effects on the cake properties and the filter performance. These include the *skin effect*, where most of the resistance of the cake becomes confined to a thin skin adjacent to the filtration medium, an insensitivity to operating variables, and a sensitivity to the operating path taken to reach the operating point. This last aspect is of special significance in the control of filtration systems, since the filter *remembers* the worst conditions that it was exposed to and performs accordingly irrespective of subsequent operational changes to improve it. This dependence of the filters performance on the operational path is due to the irreversibility of hydraulic compression. Irreversibilities due to hydraulic compression were not previously comprehensively studied in the literature.

Methods to characterise the compression-permeability-voidage (CPV) relationships for a cake have been investigated. The theory, apparatus and experimental procedure for three characterisation tests were presented, viz. the compression-permeability (C-P) cell, the settling test and the centrifuge test. The tests were then performed on a waterworks clarifier sludge to determine their applicability and ease of implementation. All tests yielded results with meaningful trends. The results for the centrifuge tests were somewhat inconsistent with those of the C-P cell and the settling tests, calling the validity of that method into question. The repeatibility of the settling test was good, but there was some scatter in the results obtained in the C-P cell tests.

The basic equations for planar, internal cylindrical and external cylindrical filtration were presented together with a solution algorithm. The equations for the internal cylindrical filtration of compressible cakes were not previously reported in the literature and were developed during the course of this project. The use of the equations was illustrated. The CPV data for the waterworks clarifier sludge was utilised to predict the performance of a planar filter and an internal cylindrical filter. These predictions were compared to results experimentally obtained on a bomb filter and the tubular filter press. A very good correlation was found between predicted and experimental filtrate fluxes and average cake solids contents. The predicted values are closer to the experimental values when only the CPV data from the C-P cell and the

settling tests are used, excluding the data from the centrifuge tests. Overall, the study indicated that a good prediction of filter performance may be obtained from employing sludge characterisation data in the appropriate filtration equations.

4 RECOMMENDATIONS

The results of the study indicate that the performance of filters may be reasonably predicted from basic sludge characterisation data. Recommendations arising from the study mainly concern methods to make these techniques more accessible to workers in the filtration field :

(i) For various reasons, workers may not be able to accurately perform the sludge characterisation tests. However, most plants monitor the performance of their filters. The feasibility of extracting compression-permeability-voidage data from operation plant data should be investigated. The data may then be used in the optimisation of the operation of the plant.

(ii) Even if the sludge characterisation data is available, the solution of the filtration equation requires numerical solution techniques that may not be readily available to workers. It is recommended that the solution procedures be coded into the form of a *user friendly* computer package which, together with a detailed Guide on sludge characterisation, should make the methodology developed in this study available to a wider audience.

ACKNOWLEDGEMENTS

The work in this report was funded by the Water Research Commission, for a project entitled *Research on the Filtration of Compressible Cakes*

The investigation was guided by a Steering Committee, which, over the period of the project, consisted of the following people:

Dr O O Hart	Water Research Commission
Professor C A Buckley	University of Natal, Durban
Mr R J J Egenes	University of Natal, Durban
Mr C M Howarth	Durban Corporation
Dr G E Rencken	US Filter
Mr G W Richardson	Durban Corporation
Dr G Offringa	Water Research Commission
Mr M Pryor	Umgeni Water

The financing of the project by the Water Research Commission, and the contribution by the members of the Steering Committee are gratefully acknowledged.

settling tests are used, excluding the data from the centrifuge tests. Overall, the study indicated that a good prediction of filter performance may be obtained from employing sludge characterisation data in the appropriate filtration equations.

4 RECOMMENDATIONS

The results of the study indicate that the performance of filters may be reasonably predicted from basic sludge characterisation data. Recommendations arising from the study mainly concern methods to make these techniques more accessible to workers in the filtration field :

(i) For various reasons, workers may not be able to accurately perform the sludge characterisation tests. However, most plants monitor the performance of their filters. The feasibility of extracting compression-permeability-voidage data from operation plant data should be investigated. The data may then be used in the optimisation of the operation of the plant.

(ii) Even if the sludge characterisation data is available, the solution of the filtration equation requires numerical solution techniques that may not be readily available to workers. It is recommended that the solution procedures be coded into the form of a *user friendly* computer package which, together with a detailed Guide on sludge characterisation, should make the methodology developed in this study available to a wider audience.

ACKNOWLEDGEMENTS

The work in this report was funded by the Water Research Commission, for a project entitled *Research on the Filtration of Compressible Cakes*

The investigation was guided by a Steering Committee, which, over the period of the project, consisted of the following people:

Dr O O Hart	Water Research Commission
Professor C A Buckley	University of Natal, Durban
Mr R J J Egenes	University of Natal, Durban
Mr C M Howarth	Durban Corporation
Dr G E Rencken	US Filter
Mr G W Richardson	Durban Corporation
Dr G Offringa	Water Research Commission
Mr M Pryor	Umgeni Water

The financing of the project by the Water Research Commission, and the contribution by the members of the Steering Committee are gratefully acknowledged.

Table of Contents

LIST OF FIGURES

LIST OF TABLES

NOMENCLATURE

A	=	area of filter medium, (m^2)
A_c	=	area of cake in C-P cell, (m^2)
α	=	empirical constant in equation (3.57)
B	=	empirical constant in set of equations (3.33)
b	=	empirical constant in equation (3.57)
C	=	empirical constant in set of equations (3.34)
F	=	empirical constant in set of equations (3.32)
F_c	=	solids compressive force, (N)
F_s	=	accumulated frictional drag on particles, (N)
H	=	height of interface between supernatent liquid and sediment, (m)
H_i	=	initial height of uniform suspension in cylinder, (m)
H_∞	=	final equilibrium height of sediment, (m)
K	=	local permeability of cake or sediment, (m^2)
K_i	=	permeability of cake when $P_s \leq P_{si}$, (m^2)
K_o	=	permeability of cake when $P_s = 0$, (m^2)
k_o	=	coefficient of earth pressure at rest, (-)
L	=	thickness of filter cake (planar filtration), (m)
n	=	empirical constant in set of equations (3.34) (compressibility coefficient)
n_1	=	empirical constant in equation (3.37)
P	=	applied filtration pressure, (Pa)
P_a	=	empirical constant, (Pa)
P_L	=	liquid pressure, (Pa)
P_s	=	solids compressive pressure, (Pa)
P_{sf}	=	solids compressive pressure corresponding to porosity of feed sludge, (Pa)

P_{si} = solids compressive pressure below which permeability, porosity and specific filtration resistance of cake are assumed constant, (Pa)

P_{sm} = solids compressive pressure at filter medium, (Pa)

P_l = liquid pressure at medium, (Pa)

ΔP_c = pressure drop across the cake, (Pa)

ΔP_m = pressure drop across the medium, (Pa)

Q = overall volumetric flow rate of liquid (filtrate) per unit length of filter tube, ($m^3/m.s$)

Q_f = overall volumetric flow rate of liquid (filtrate), (m^3/s)

q_2 = empirical constant

R_c = distance between centre of centrifuge and bottom of centrifuge tube, (m)

R_m = resistance of medium, (m^{-1})

r = radius, (m)

r_c = distance from centre of centrifuge, (m)

r_l = distance from centre of centrifuge to surface of sediment, (m)

r_r = square root of the correlation coefficient, (-)

r_t = radius of centrifuge tube, (m)

r_1 = internal radius of filter medium, (m)

r_2 = internal radius of cake, (m)

Δr_c = thickness of differential element of sediment, (m)

t = time, (s)

Δt = time interval, (s)

Δt_c = thickness of cake in C-P cell, (m)

u = superficial velocity of liquid (filtrate), (m/s)

V = volume of filtrate per unit length of tube, (m^3/m)

v = volume of filtrate per unit medium area, (m^3/m^2)

v_o = initial settling velocity of surface of sediment, (m/s)

W = total mass of dry solids in cake, (kg)

w = mass of cake dry solids per unit medium area deposited in thickness x from medium (planar filtration), (kg/m^2)

w_c = total mass of cake dry solids deposited per unit medium area, (kg/m^2)

x = distance from medium for planar filtration, (m)

y = distance measured from bottom of cylinder, (m)

y_m = distance from membrane or filter medium, (m)

z = mass fraction of moisture in cake, (-)

GREEK SYMBOLS

α = local specific filtration resistance of cake or sediment, (m/kg)

α_{av} = average specific filtration resistance of cake, (m/kg)

α_i = specific filtration resistance of cake when $P_s \leq P_{si}$, (m/kg)

α_o = specific filtration resistance of cake when $P_s = 0$, (m/kg)

β = empirical constant in set of equations (3.33)

β_1 = empirical constant in equation (3.36)

δ = empirical constant in set of equations (3.32)

δ_1 = empirical constant in equation (3.35)

ϵ = local porosity of cake or sediment, (-)

ϵ_{av} = average porosity of cake, (-)

ϵ_f = porosity of feed sludge, (-)

ϵ_i = porosity of cake when $P_s \leq P_{si}$, (-)

ϵ_{if} = internal porosity of particle aggregates, (-)

ϵ_{in} = initial porosity of suspension, (-)

ϵ_L = lower limit of porosity for dilute region where free or hindered settling of particle aggregates occurs, (-)

ϵ_o = porosity of cake when $P_s = 0$, (-)

θ = cylindrical co-ordinate in cylindrical filtration, (radians)

μ = viscosity, (Pa.s)

μ_f = viscosity of liquid (filtrate), (Pa.s)

ρ_l = liquid density, (kg/m^3)

ρ_s = solids density, (kg/m^3)

ϕ = volume fraction of particles, (-)

ϕ_s = volume fraction of solids in feed sludge, (-)

Ω = angular velocity, (rad/s)

ω = volume of dry solids per unit cross-sectional area of tube or cylinder measured from bottom of tube or cylinder, (m^3/m^2)

ω_c = volume of cake dry solids per unit medium area, (m^3/m^2)

ω_o = total volume of dry solids per unit cross-sectional area of tube or cylinder, (m^3/m^2)

ABBREVIATIONS

C-P = Compression-Permeability

CFMF = cross-flow microfiltration

CPV = compression-permeability-voidage data

TFP = tubular filter press

Chapter 1

INTRODUCTION

1.1 BACKGROUND

WRC Project No. 238, *Design Criteria for Cross-flow Microfiltration*, was initiated in 1987. The main objectives of that project were to determine the fundamental mechanisms that govern the behaviour and performance of high-velocity cross-flow microfiltration (CFMF) and the tubular filter press (TFP). The Water Research Commission has a licensing agreement with HTW High Tech Water NV with respect to CFMF and TFP technologies.

Initial work focussed on investigations into the fluid and particle dynamics in those systems. It soon became apparent that the system behaviours were to a significant extent determined by the behaviour of the cake, and in particular, with effects associated with compression of the cake. It was realised that a knowledge of compressible cakes would be of benefit to the water industry at large, in addition to the *Design Criteria for Cross-flow Microfiltration* Project. Hence, the current project was motivated, to investigate effects associated with compressible cakes, methods to characterise compressibility and methods to predict the performance of systems where compressible cakes exist.

In the initial project motivation, the ambit was to utilise compression-permeability (C-P) cells to characterise the compressibility of sludges. However, investigations indicated that C-P cells alone would be inadequate to characterise sludges at low solids compressive pressures. Data at low compressive pressures is of importance in highly compressible cakes. Accordingly, the ambit of the project was extended to include investigations into alternative characterisation methods for low solids compressive pressures. In a further extension to the ambit of the project, methodology to predict the performance of three common filter geometries, viz. planar, internal cylindrical and external cylindrical, have also been investigated and developed.

1.2 DEFINITION OF PROBLEM, AIMS AND OBJECTIVES

Filtration is widely employed in the water industry, for the clarification of suspensions, the concentration of suspensions and the dewatering of sludges. The most significant indicators of filter performance are the rate of production of filtrate and the properties of the final cake, i.e. its moisture content and degree of consolidation. The latter performance indicator is of particular significance in sludge dewatering applications.

In most instances, the cakes formed are compressible, i.e. it undergos changes to its structure and properties during the filtration process. This can significantly affect the performance indicators, as well as introduce seemingly spurious system behaviours. Accordingly, in order to design, operate and optimise filtration systems, it is necessary to have a knowledge of the effects that compressible cakes have on systems.

The aim of this study is to acquaint workers in the water field with the effects associated with compressible cakes, and to identify and develop methodology that would enable workers to characterise compressible cakes and predict the performance of large scale filters from laboratory tests.

In order to predict the performance parameters for compressible cake systems, it is necessary to characterise the compressibility of the cake, and to employ this in filtration equations appropriate to the geometry of the filter.

Various methods to characterise cake compressibility have been reported in the literature, ranging from tests based on simple theory, e.g. the Buchner Funnel Test, to those based on fairly elaborate theory, e.g. settling tests. However, there are often contradictory claims regarding their validity and applicability. In addition, experimental equipment and procedures are often not clearly stated, leading to poor repeatability in characterisation tests. Hence, it is necessary to investigate these methods, evaluate them, and summarise them into a form that may easily be employed by workers in the filtration field.

Filter geometries may be divided into three categories :

(i) planar - e.g. plate and frame filters, leaf filters, belt filters and rotary vacuum filters. Although rotary filters are strictly cylindrical, the cake formed may be regarded as planar, since the thickness of the cakes is invariably small compared to the diameter of the filter.

(ii) external cylindrical filtration e.g. candle filters

(iii) internal cylindrical filtration e.g. the tubular filter press.

The basic filtration equations for planar filtration are widely reported in the literature. Equations for the filtration of compressible cakes on external cylindrical surfaces have been reported, but do not enjoy widespread application. This could, in part, be due to a lack of knowledge of the importance of compressible cakes and a lack of design methodology. Equations for the filtration of compressible cakes on internal cylindrical surfaces have not been developed. Hence, noting that the TFP is a major part of the *Design Criteria for Crossflow Microfiltration* project, it is necessary to develop the appropriate equations and solution procedures for filtration on internal cylindrical surfaces.

Accordingly, the objectives of this project are as follows :

(i) to investigate the mechanisms responsible for compressible cake behaviour,

(ii) to investigate the effects that compressible cakes have on filtration systems,

(iii) to investigate methods to characterise cake compressibility,

(iii) to identify and develop models and equations to predict filtration performance for compressible cake systems.

1.3 ORGANISATION

In Chapter 2, the mechanisms governing the compression of cakes are discussed. The major cause of compression in filters, *hydraulic compression*, is outlined. The effects that hydraulic compression have on the properties of the cake are discussed.

Chapter 3 concerns the characterisation of cake compressibility, and specifically addresses the quantification of permeability/compressive pressure and voidage/compressive pressure relationships. Hereafter, compressive pressure-permeability-voidage relationships will be referred to as CPV data. Models to correlate CPV data are outlined. The theory, apparatus and procedures for three laboratory tests are discussed, viz. the compression-permeability (C-P) cell, the settling test and the centrifuge test. These tests are then applied to obtain CPV data for a waterworks clarifier sludge. The validity and possible applicability of the three tests are discussed in terms of the results obtained.

Chapter 4 illustrates the utilisation of CPV data to predict filter performance. The filtration equations for planar, internal cylindrical and external cylindrical filtration are presented, together with a solution algorithm. The CPV data obtained in section 4 is utilised to predict the filtrate flux - time relationship and the average cake solids for planar and internal cylindrical filtration. This is compared to constant pressure experimental fluxes and cake solids contents obtained on a planar filter and the TFP.

In Chapter 5, the major findings of this work are stated, and in Chapter 6 recommendations for future work are made.

Chapter 2

THEORY OF COMPRESSIBLE CAKES

2.1 GENERAL THEORY OF COMPRESSION

Firstly, the distinction between *cake* and *suspension* must be drawn. This distinction may be visualised by considering how the mobility or fluidity of a flowing suspension changes as its concentration is increased. With increasing concentration, the mean distance between particles decreases, particle-particle interactions increase and the viscosity of the suspension increases. Each particle is however, still suspended in the flowing fluid. Further increases in concentration will result in further decreases in the mean inter-particle distance until at some critical condition particles will be fully bounded by other particles i.e. the particles will have reached some critical packing density, closely corresponding to the maximum random packing density[1] . Now, in contrast to being suspended in a flowing fluid, the particles form a coherent, stable structure which is permeated by the flowing fluid. This structure can be regarded as cake.

Formally then, cake may be defined as particles at a concentration corresponding to the maximum random packing density for the specified size distribution and particle shape. In the case of compressible cakes, the packing density will be a strong function of the solids compressive pressure. In this instance the minimum concentration that can be regarded as cake will be that concentration corresponding to the random packing density at zero consolidation pressure.

The flow of fluid through a porous cake may be described by D'Arcy's equation :

$$\Delta P_c = \frac{\mu \; u \; \Delta x}{K} \qquad (1)$$

where ΔP_c = pressure drop across a cake of thickness Δx (Pa)

μ = fluid viscosity (Pa.s)

u = superficial fluid velocity through cake (m/s)

K = local cake permeability (m^2)

The permeability, K, is a function of the particle size distribution and particle shape. It is related to the specific cake resistance (α) of the cake by :

$$K = \frac{1}{\alpha \; \rho_s \; (1-\epsilon)} \qquad (2)$$

1 For "ideal" particles, where physio-chemical interactions between particles are negligible, this critical concentration may occur when the particles physically touch each other. For systems where significant physio-chemical interactions occur, e.g. flocs and particles that have a significant layer of bound water sttached to them, the critical concentration may occur well before the particles actually come into contact with each other.

where ρ_s = particle density (kg/m^3)

ϵ = cake voidage (volumetric fraction of cake occupied by voids)

Each cake structure is capable of withstanding some compressive stress. If the structure can withstand a very high compressive stress without experiencing a rearrangement, the cake is said to be incompressible. Examples of these would be cakes formed from uniformly sized spheres. In this instance, the voidage in the cake and its permeability are not affected by the application of compressive stresses. Most real cakes however experience a change to their structure over a wide range of compressive stresses, and are said to be compressible. Compressive stresses may arise from the unbuoyed weight of solids in thickeners, radial acceleration in centrifuges, and frictional forces in filtration. In this instance, a rearrangement of the cake particles occurs under the action of the compressive stresses, leading to a more densely packed cake with a decreased voidage and a decreased permeability. It should be noted that the decreased voidage and permeability arises from collapsing particulate structures in the cake, and not from the deformation of individual particles.

The compressibility of the cake is indicated by how the voidage and the permeability change with compressive pressure. Typical trends exhibited by incompressible, moderately compressible and highly compressible cakes are depicted in Figure 1.

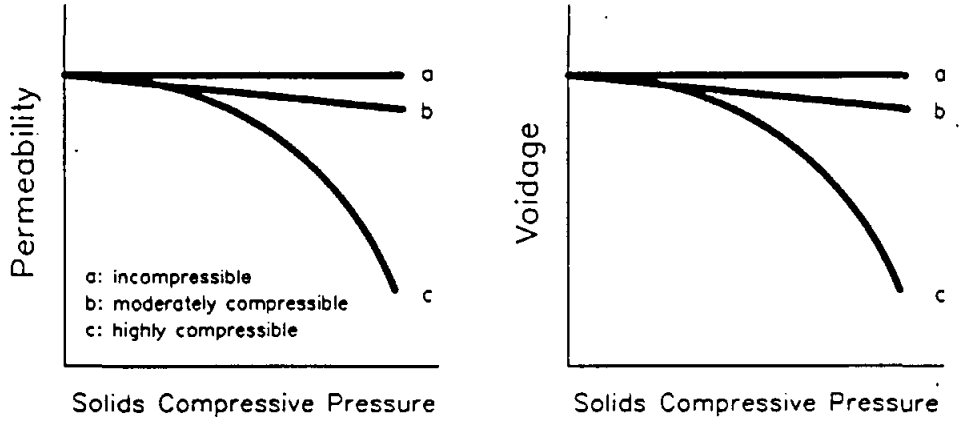

FIGURE 1 **Qualitative Effect of Solids Compressive Pressure on Permeability and Voidage**

In filtration, compression of the cake arises primarily from hydraulic frictional forces, and is termed *hydraulic compression.*

2.2 HYDRAULIC COMPRESSION

The flow of fluid through a cake consisting of particles of a wide range of sizes could cause a rearrangement of the particulate structure, leading to a cake of decreased voidage [Tiller and Yeh (1987)]. This process is termed *hydraulic compression* and arises by smaller particles being forced into the existing void spaces by fluid drag forces, yielding a more densely packed cake of reduced voidage and permeability. It must be noted that this compression of the cake is not due to the deformation of individual particles, but to a re-arrangement of the particles.

In the discussion that follows, the force balances refer to cakes formed on planar surfaces. The force balances for cakes formed on cylindrical surfaces will be addresses in Section 4.1.

In cake filtration, solid particles form a filter cake on the filter medium, and liquid flows through the interstices of the cake in the direction of decreasing liquid pressure. Each particle is subjected to frictional drag due to flow of the liquid. The forces on the particles are communicated from particle to particle at points of contact.

Since the solid particles are assumed to be in point contact, the liquid pressure, P_L, is effective over the entire cross-sectional area, A (Leu, 1981). The forces acting on a differential element, dx, of the filter cake are shown in Figure 2. The following equation may be derived from Newton's second law of motion, assuming that inertial effects and acceleration are negligible in filtration (Tiller et al., 1986) :

$$dF_s + AdP_L = 0 \tag{3}$$

where F_s = accumulated frictional drag on particles (N)

The solids compressive pressure is defined as :

$$P_s = \frac{F_s}{A} \tag{4}$$

Therefore from equation (3) :

$$dP_s + dP_L = 0 \tag{5}$$

or

$$\frac{dP_s}{dx} + \frac{dP_L}{dx} = 0 \tag{6}$$

where x = distance from medium for planar filtration (m)

Equations (5) and (6) state that the frictional drop of the liquid is offset by a corresponding increase in the solids compressive pressure.

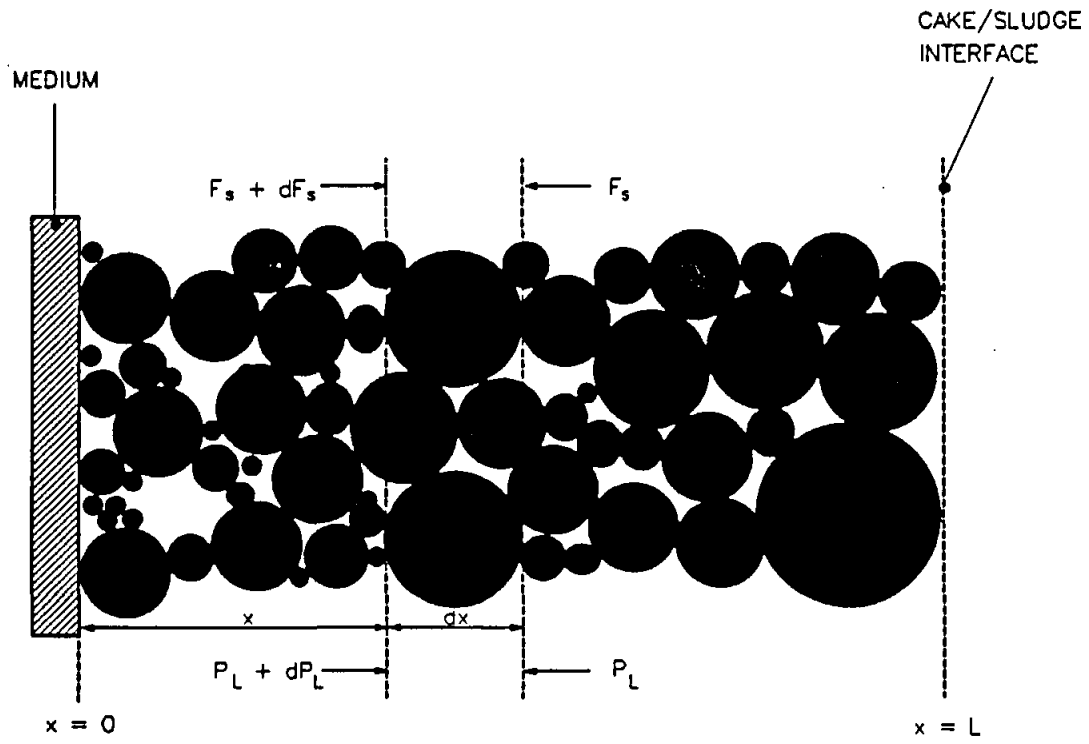

FIGURE 2 **Diagram Showing the Forces Acting on a Differential Element of Cake for Planar Filtration**

The variation of liquid pressure and solids compressive pressure is shown in Figure 3 for planar filtration. In Figure 3 the following boundary conditions apply :

P_L at cake/sludge interface	$= P$
P_L at medium	$= P_1$
P_s at cake/sludge interface	$= 0$
P_s at medium	$= P - P_1$.

where P_1 = liquid pressure at medium (Pa)

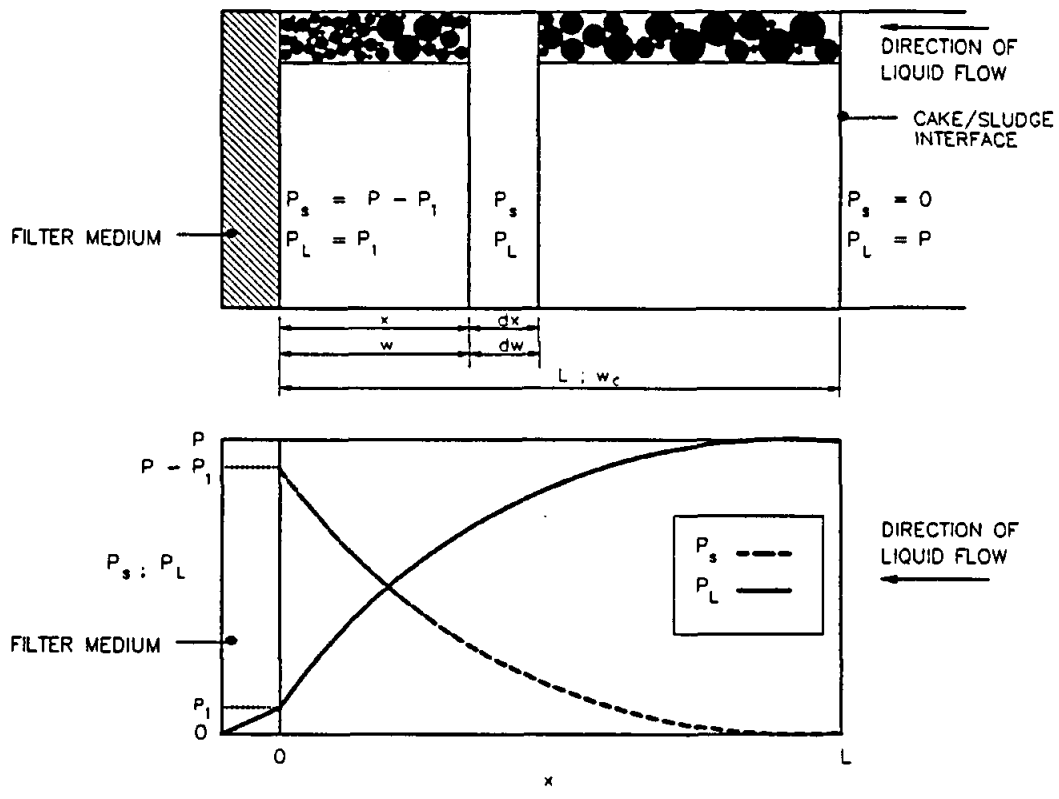

FIGURE 3 **Schematic Diagram of a Filter Cake and its Liquid and Solids Compressive Pressure Profiles for Planar Filtration**

The hydraulic pressure, P_L, is a maximum at the cake surface and progressively decreases towards the medium, due to fluid drag losses. The solids compressive pressure, P_s, is zero at the cake surface and progressively increases towards the support medium as the cumulative drag forces experienced by the particles increase.

This hydraulic compression of the cake is highly irreversible i.e. if P_s at a point is now decreased, e.g. by decreasing the fluid flow through the cake, particles cannot retrace paths out of the void spaces, and hence the voidage will remain at the level determined by the higher P_s. As a cake grows, the P_s and P_L profiles will change. However, particles at any point in the cake will always be exposed to an increasing P_s (Figure 4).

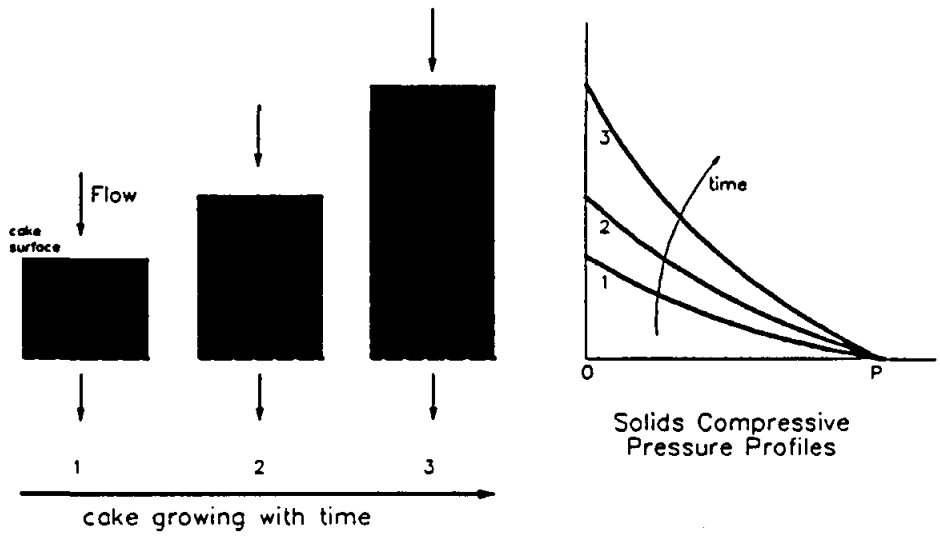

FIGURE 4 **Change in Solids Compressive Pressure Profiles as Cake Grows**

This variation in solids compressive pressure through the cake has three significant effects on the cake :- variations in voidage through the cake, variations in the local permeability and variations in the resistance to tangential shears.

2.2.1 Variations in Voidage

From Figure 1 and Figure 3, it is seen that the variation in solids compressive pressure through the cake will result in a variation in the voidage. Typical voidage profiles for incompressible, moderately compressible and highly compressible cakes are shown in Figure 5.

For highly compressible cakes, it is seen that the voidage near the filter medium is low, and can increase drastically as the surface of the cake is approached. This indicates that the surface layers would be loosely packed and have a very high moisture content while the layers near the medium would be more consolidated.

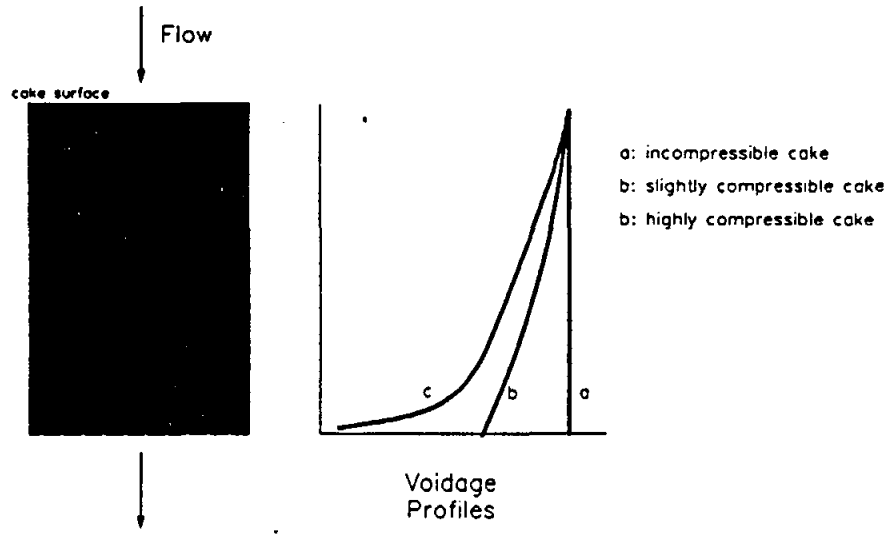

FIGURE 5 **Voidage Profiles Resulting from Hydraulic Compression of the Cake**

2.2.2 Variations in Permeability

From Figure 1 and Figure 3 it is seen that permeability profiles will be established through the cake. Typical are shown in Figure 6 for slightly compressible and highly compressible cakes. A major significance of this permeability profile is that most of the overall cake resistance is offered by cake layers closer to the wall. On moving away from the wall, the contribution that each layer makes to the overall cake resistance progressively decreases.

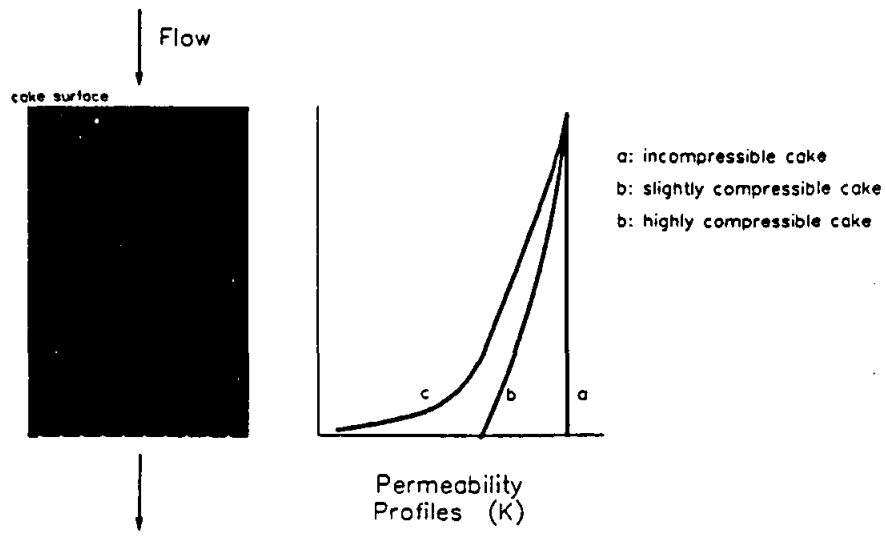

FIGURE 6 **Permeability Profiles Resulting from Hydraulic Compression of Cake**

2.2.3 Variations in Resistance to Tangential Shears

In the TFP and CFMF, the cake is subjected to a tangential stress caused by the motion of the bulk fluid. This tangential stress tends to shear off layers of the cake that have already been formed. Cakes formed in planar filters are also subjected to tangential stresses, during the transportation, handling and storage of the cakes. Here too, the tangential stresses tend to cause fracture and destruction of the cakes. Hence, the resistance of a cake to fracture by tangential shears is of importance.

The particles in any given layer in a cake experience inter-particle attractive forces with neighbouring particles (i.e. *particle friction*), which enables the layer to resist fracture due to tangential stresses. Accordingly, for each layer in a cake, the tangential stress on the layer must exceed some critical value before the layer will fracture. This may be termed the critical shear stress, τ_{crit}. The inter-particle forces on a layer will increase as the solids compressive pressure on that layer increases and the voidage decreases. Hence, τ_{crit} will be a positive function of the solids compressive pressure, i.e.

$$\tau_{crit} = function\left(P_s^{q_2}\right) \tag{7}$$

where q_2 = a constant (>0)

This is analogous to the *powder yield locus* in soil mechanics, where the critical shear stress for failure in a powder is a function of the compressive stress being experienced by the powder [Smith (1982)].

From equation 7 and Figure 3, it is seen that hydraulic compression of the cake will cause a τ_{crit} profile to be established through the cake (Figure 7).

The major implication of Figure 7 is that in a highly compressible cake, the surface layers will be poorly consolidated, and will be easily sheared off.

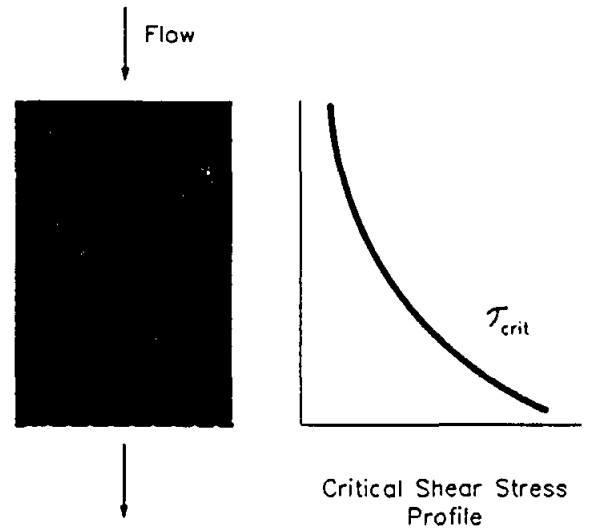

FIGURE 7 **Critical Shear Stress Profile Resulting from Hydraulic Compression of Cake**

2.3 EFFECTS CAUSED BY HYDRAULIC COMPRESSION

2.3.1 Skin Effect

From Figure 6, it is seen that for highly compressible cakes most of the resistance to flow is confined to a thin skin immediately next to the filtration medium. The solids compressive pressure in this skin is high, and the skin is densely packed and well consolidated. Over the rest of the cake however, the solids compressive pressure is relatively low. Hence the majority of the cake has a high voidage, and hence high moisture content, and is not very well consolidated.

One implication of this skin is that the average solids content of the cake will be low. Attemps to increase the solids content by, e.g., operating at a high pressure are likely to be ineffective, since this will merely result in a slight increase in the thickness of the skin, and will not

significantly affect the overall cake. Indeed, the average cake solids content may increase if the filter is operated at a *lower* pressure. This may be ascertained by predicting the voidage profiles for different operating pressures.

The second significant implication of the skin is that the majority of the cake, and especially the surface layers, will be poorly consolidated and have a low critical shear stress (see Section 2.2.3). This indicates that the surface layers will be easily sheared off, and has important implications for the transport and storage of such cakes.

In order to choose an operating point that minimises the effect of the skin, it is necessary to predict the voidge and solids compressive pressure profiles through the cake. The methodology to achieve this is discussed in Chapter 4.

2.3.2 Insensitivity to Operating Variables

For an incompressible cake, the filtrate flux will increase linearly with the operating pressure. For highly compressible cakes, however, increases in pressure may result in equivalent increases in cake resistance, so that the filtrate flux is independent of operation pressure (Tiller and Yeh, 1987). This indicates that the extra energy involved in operating at higher pressures is being used to express liquid from the skin, and not in increasing the production rate of the filter. In compressible cakes therefore, operating at a higher pressure will not necessarily yield a higher production rate. This was observed in filtration experiments performed on a waterworks clarifier sludge in this study (see Section 4.2). Indeed, in some CFMF applications, it has been found that production rates decrease with pressure (see Pillay, 1992).

2.3.3 Dependence of Filtrate Flux on Operating Path

Hydraulic compression is an highly irreversible process. If a cake is exposed to a high compressive pressure it undergos an irreversible structural change to form a more densely packed structure, of reduced voidage and increased resistance to flow. This structure is maintained even if the solids compressive pressure is subsequently reduced. Hence if a cake is exposed to a high compressive pressure it maintains the resistance appropriate to the higher pressure even if the pressure is subsequently lowered. Effectively, the system *remembers* the worst conditions that it was exposed to.

This has significant implications for the operation of filters, since the performance factors now become dependent on the history of the filters operating path. Consider, for example, a filter that is designed to operate at 300 kPa. If, due to poor control, the filter is exposed to a higher pressure for a significant time, solids compressive pressure, voidage and permeability profiles appropriate to the higher pressure will be established. In effect, the overall resistance of the cake will increase. If the pressure is now corrected back to 300 kPa, the cake maintains the higher resistance. Hence, the filtrate production rate will be lower than that obtained if the cake had not been subjected to the higher pressure.

This dependence of the filter's performance on the operating path has been comprehensively studied in cross-flow microfiltration (see Pillay, 1992). For example, it was observed that starting up a CFMF at a low velocity, running for some time at the low velocity, and then increasing the velocity yields a significantly lower filtrate flux than if the system were started up at the higher velocity. Similar, seemingly spurious, behaviours were also observed when the system is subjected to step changes in pressure and concentration. This behaviour is completely explicable in terms of irreversible compression of the cake.

The dependence of filtrate flux on the operating path emphasises the necessity for better control of filtration systems.

Chapter 3

CHARACTERISATION OF COMPRESSION-PERMEABILITY-VOIDAGE (CPV) DATA

Characterising the compressibility resolves to determining how the voidage and permeability (or specific cake resistance) change with solids compressive pressure. To date, no method exists to predict CPV data from basic particle properties, i.e. size distribution, shape and density. Various models have been proposed to *correlate* CPV data. However, model parameters must still be determined from suitable laboratory tests on the suspension.

The most widely known method to obtain an *indication* of cake resistance is the standard Buchner Funnel test. This is fairly useful to obtain an indication of the *relative* resistances of cakes (WRC Report No. 89/1/85), but is not of value in obtaining detailed compression-permeability data to predict cake profiles and properties. The major flaw of the test is that the cake undergos hydraulic compression during the test, establishing a solids compressive pressure profile through the cake. Hence, the specific cake resistance obtained from the test represents some average value for the cake and does not yield detailed information on the true CPV relationship.

Another widely known test is the compression-permeability (C-P) cell test. This does yield information on the relationships between permeability, voidage and compressive pressure. However, the C-P cell test is also subject to limitations. For a very compressible cake (like the cake formed from the waterworks sludges) a highly resistant layer or skin is formed near the medium (Tiller and Green, 1973), while the bulk of the cake is not very well consolidated. The solids compressive pressure is relatively low in this "sloppy" cake region. Therefore, for very compressible cakes it is important to have accurate data in the relatively low solids compressive pressure region.

Although C-P cells have been used down to very low solids compressive pressures, for example down to 2 kPa by Tiller and Cooper (1962), serious reservations have been expressed by many authors on the accuracy of the C-P cell data in the low solids compressive pressure region (e.g. Shirato et al., 1983 and Tiller and Lu, 1972). The main reason for inaccurate results is friction between the inner wall of the C-P cell and the compressed cake.

Shirato et al. (1983) proposed a batch settling technique for the determination of porosity and permeability at very low solids compressive pressures. Shirato et al. (1983) obtained porosity

data for three different sludges (zinc oxide, Mitsukuri Gairome clay and ferric oxide) for the P_s range, $100\ Pa \leq P_s \leq 1\,000\ Pa$. Permeability data for the same sludges were determined for the P_s range, $0{,}1\ Pa \leq P_s \leq 100\ Pa$.

Murase et al. (1989) proposed a centrifuge method for the determination of porosity data for intermediate solids compressive pressures. Murase et al. (1989) obtained porosity data for zinc oxide and ferric oxide slurries for the P_s range, 1 000 Pa $< P_s <$ 100 000 Pa.

Since the cake obtained from the waterworks clarifier sludge which was used for this study, was very compressible, it was decided to use all three methods (i.e. settling (low P_s); centrifuge (intermediate P_s) and C-P cell (high P_s)) in order to obtain porosity and permeability data over a wide range of solids compressive pressures.

In this Chapter, methods to quantify CPV data are investigated. In Section 3.1 various models proposed to correlate data are presented. In Section 3.2 the theory, experimental apparatus and experimental procedure for the C-P cell test, settling tests and centrifuge tests are discussed. In Section 3.3 these tests are applied to obtain CPV data for a waterworks clarifier sludge.

3.1 MODELS

Tiller and Cooper (1962) proposed the following equations to relate permeability (K), porosity (ϵ) and specific cake resistance (α) to solids compressive pressure :

$$\begin{aligned} K &= FP_s^{-\delta} && P_s \geq P_{si} \\ K &= K_i = FP_{si}^{-\delta} && P_s \leq P_{si} \end{aligned} \tag{8}$$

$$\begin{aligned} (1-\epsilon) &= BP_s^{\beta} && P_s \geq P_{si} \\ (1-\epsilon_i) &= BP_{si}^{\beta} && P_s \leq P_{si} \end{aligned} \tag{9}$$

$$\begin{aligned} \alpha &= CP_s^{n} && P_s \geq P_{si} \\ \alpha &= \alpha_i = CP_{si}^{n} && P_s \leq P_{si} \end{aligned} \tag{10}$$

where B = empirical constant in set of equations (9)

C = empirical constant in set of equations (10)

F = empirical constant in set of equations (8)

K_i = permeability of cake when $P_s \leq P_{si}$, (m^2)

n = empirical constant in set of equations (10) (compressibility coefficient)

P_{si} = solids compressive pressure below which permeability, porosity and specific filtration resistance of cake are assumed constant, (Pa)

α_i = specific filtration resistance of cake when $P_s \leq P_{si}$, (m/kg)

β = empirical constant in set of equations (9)

δ = empirical constant in set of equations (8)

ϵ_i = porosity of cake when $P_s \leq P_{si}$, (-)

There is some experimental evidence that permeability, porosity and specific filtration resistance are constant below some low solids compressive pressure, P_{si} (Tiller and Leu, 1980). According to Tiller and Leu (1980) the location of P_{si} is entirely empirical and relatively arbitrary, the main problem being that Compression-Permeability (C-P) cells (see section 3.2.1) are not very accurate at the low solids compressive pressures required to locate P_{si} accurately.

Tiller and Leu (1980) proposed the following set of alternative empirical equations :

$$K = K_o\left(1 + \frac{P_s}{P_a}\right)^{-\delta_1} \tag{11}$$

$$1 - \epsilon = (1 - \epsilon_o)\left(1 + \frac{P_s}{P_a}\right)^{\beta_1} \tag{12}$$

$$\alpha = \alpha_o\left(1 + \frac{P_s}{P_a}\right)^{n_1} \tag{13}$$

where K_o = permeability of cake when $P_s = 0$, (m^2)

n_1 = empirical constant in equation (13)

P_a = empirical constant, (Pa)

α_o = specific filtration resistance of cake when $P_s = 0$, (m/kg)

β_1 = empirical constant in equation (12)

δ_1 = empirical constant in equation (11)

ϵ_o = porosity of cake when $P_s = 0$, (-)

From equations (8) to (13), it is seen that various parameters must be ascertained in order to employ the correlative equations. Methods to determine these compressibility parameters are discussed in the next section.

3.2 THEORY, APPARATUS AND PROCEDURE

3.2.1 Compression-Permeability (C-P) Cell

3.2.1.1 Theory of Operation

The basic principle of the C-P cell is that a sample of the cake is *MECHANICALLY* compressed to a chosen pressure, whereafter the permeability of the cake is measured. The mechanical compression of the cake ensures that the entire cake is subjected to the same solids compressive pressure, i.e. there are no P_s profiles as in hydraulic compression. In effect, the sample in the C-P cell represents a differential slice through a hydraulically compressed cake.

A concentrated slurry of the material to be tested is inserted into the cell. The slurry is then mechanically compressed by the action of a piston or a pressurised rubber diaphragm. During this mechanical compression, fluid is expressed out of the slurry and a cake is formed. The cake structure then undergos a rearrangement until the consolidation appropriate to the compressive pressure is obtained. Fluid under a known pressure is allowed to permeate through the consolidated cake and the rate of permeation is measured. It may be perceived that during this permeation hydraulic compression of the cake will occur. However, the pressure of the permeating fluid is significantly lower than the mechanical compressive pressure to which the cake was exposed, and no further compression of the cake occurs during the permeation. Following the permeation measurement, the cake is then weighed, dried and reweighed, and the voidage is inferred. The process is repeated for a range of compressive pressures.

For a specified solids compressive pressure, the liquid permeability is calculated from the D'Arcy equation:

$$K = \frac{\mu \; Q_f \; \Delta t_c}{A_c \; \Delta P_c} \qquad \textit{from (1)}$$

where A_c = area of cake in C-P cell (m^2)

Δt_c = thickness of cake in C-P cell (m)

ΔP_c = pressure drop across cake (Pa)

Q_f = flowrate of filtrate through cake (m^3/s)

The specific filtration resistance, α , at a certain solids compressive pressure may be calculated from the permeability by using equation (2) :

$$\alpha = \frac{1}{\rho_s K (1-\epsilon)} \qquad \textit{from (2)}$$

The porosity of the cake at the end of a C-P cell test may be calculated from the final moisture content of the cake from the following equation :

$$\epsilon = \frac{Volume\ of\ liquid}{Volume\ of\ liquid\ +\ Volume\ of\ solids}$$

$$= \frac{z/\rho_l}{z/\rho_l\ +\ (1-z)/\rho_s} \qquad (14)$$

where z = mass fraction of moisture in cake, (-)

ρ_l = liquid density, (kg/m^3)

3.2.1.2 Apparatus and Procedure

A detailed summary of the various types of C-P cells reported in the literature is presented in **WRC Project No. 241**, *Progress Report to the Steering Committee, May 1990.*

A process schematic of the C-P cell which was used during this study is shown in Figure 8. The C-P cell was constructed according to the design given by Rowe et al. (1966). Significant features of the cell are as follows :

(i) the mechanical compression is enabled by a pressurised rubber diaphragm

(ii) the pressure of the permeating fluid is determined by a header tank. The level in the tank is maintained by an overflow line.

(iii) the permeating fluid travels down a central stem whose outlet is located below the rubber diaphragm. The base of the stem is attached via an airtight connection to the rubber diaphragm.

(iv) a dial gauge monitors the motion of the stem, and hence indicates the decreasing thickness of the cake.

A detailed diagram of the cell is given in the abovementioned Progress Report.

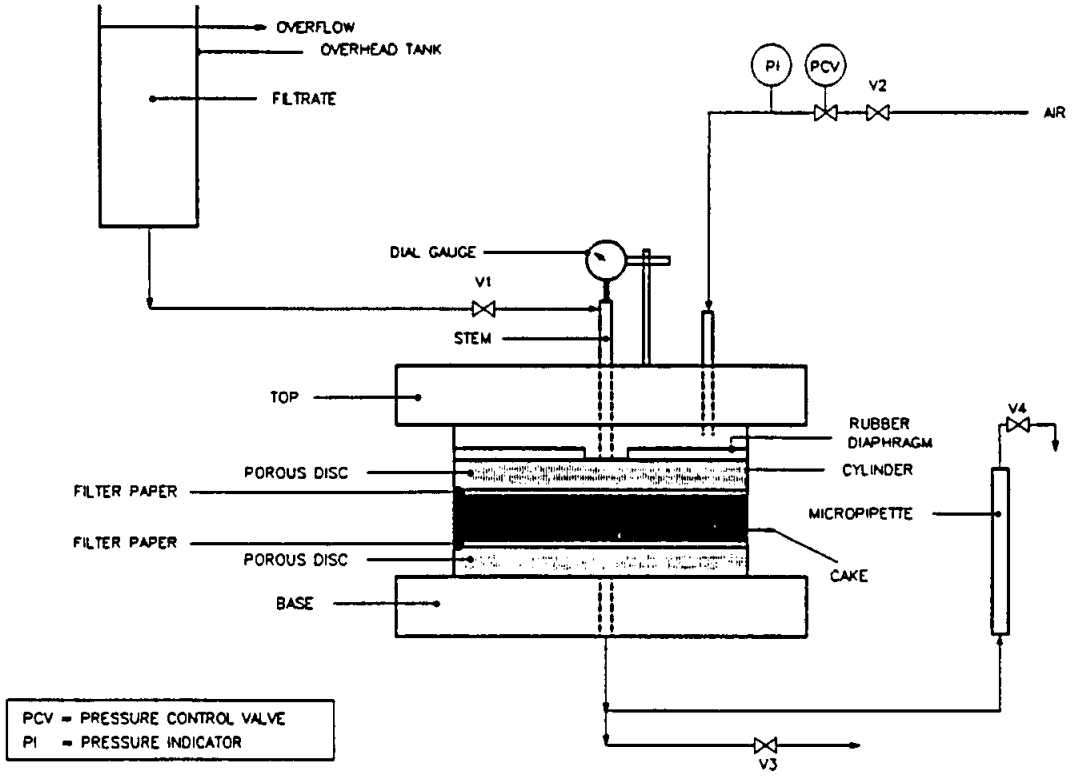

FIGURE 8 **Schematic Diagram of the Compression-Permeability (C-P) Cell**

Past experience in the laboratories of the Pollution Research Group has indicated that the repeatibility of data obtained on a C-P cell is to a great extent determined by the procedure followed in the test. Accordingly, the procedure adopted in the tests is detailed below.

The micropipette is located so that its level is approximately equal to that of the bottom flange on the C-P cell. The difference in height between the micropipette and the overflow pipe on the header tank defines the permeation head. A suspension of the test solids is prepared and allowed to settle. The supernatent is siphoned off and poured into the header tank. The excess supernatent is stored.

The cylinder is placed on the C-P cell base and partially filled with liquid. In order to obviate chemical effects, the appropriate liquid to be used in the test is the supernatent obtained earlier. Air bubbles are then expelled from the feed line to the micropipette and from the micropipette by-pass line by allowing liquid to flow through these lines. The bottom porous disc is carefully inserted and filter paper of a slightly larger diameter than the internal diameter of the cylinder is placed on top of the porous disc. Care must be taken to ensure that the filter paper forms a proper seal at its outer edge.

Valve V3 is closed and the concentrated sludge is then introduced on top of the filter paper. The cell is then partially filled with supernatent. The sludge is allowed to settle until a clear cake/liquid interface develops. A second filter paper is then introduced into the cell and allowed to settle onto the cake. It may be necessary to gently press the filter paper to ensure that the paper sits evenly and horizontally on the cake. The second porous disc is introduced into the cell. The supernatent permeates the disc, and it settles onto the second filter paper. The cylinder is then filled with liquid until overflows.

Valve V1 is opened to allow liquid to flow from the header tank through the stem, expelling air bubbles from the line. The diaphragm and top assembly is then carefully lowered onto the top of the cylinder and the top is firmly bolted onto the base thereby clamping the diaphragm between the top and the cylinder. Valve V1 is then closed. The dial gauge is fixed to the stem and its arm secured to the top of the cell.

Valve V4 is opened. The diaphragm is inflated to the desired pressure with air by opening valve V2. The air pressure is adjusted by means of the pressure control valve. Valve V3 is then opened.

As the rubber diaphragm compresses the cake, liquid is expressed and flows out of V3. The dial gauge is monitored. When the cake is fully consolidated, the motion of the dial gauge ceases. For the waterworks sludge investigated in this study, this took from 90 to 120 minutes.

When the cake is fully consolidated, valve V1 is opened. Liquid permeates the consolidated cake and exits through V3. The rate of permeation is measured by closing V3 and monitoring the rate of rise of liquid in the micropipette [1]. The rate of permeation should be measured at regular intervals until it stabilises.

At the end of the run the cell is dismantled and the cake is carefully removed and weighed. The cake is then dried 105 °C for at least 5 hours and reweighed.

The following important checks should be performed to ensure validity of the results :

(i) The test should be performed without the cake. The permeation rates thus obtained will indicate whether the porous disks, filter paper and flow lines contribute a significant resistance to the system.

(ii) On dissembling the rig, check that no slurry exists above the top porous disc. If slurry does exist, it indicates that some of the cake squirted past the top filter paper during the compression, thereby invalidating the test.

(iii) At no stage should the cake be exposed to the compressed air. This can occur if, e.g. the rubber diaphragm has developed a leak. If any air spaces develop in the cake, this will reduce the effective area for liquid permeation, and hence invalidate the test.

---

1 The permeation head will change as the level in the micropipette changes. In order to make this change insignificant, it is important to ensure that the total head is significantly greater than the fluctuation in level of the micropipette.

(ii) After the cake has been compressed, data may be obtained for various permeation heads by changing the position of the header tank. In principle the K calculated at a given compressive pressure should be independent of the head.

3.2.2 Settling Method

3.2.2.1 Theory

a Determination of Porosity

The following technique for the determination of porosities at low solids compressive pressures was developed by Shirato et al. (1983).

When a suspension containing the dry solids volume, ω_o, per unit area settles in a cylinder, the final equilibrium height of the sediment is denoted by H_∞, as shown in Figure 9(a). When the initial volume of solids is increased by the volume $d\omega_o$, as shown in Figure 9(b), the final height of the sediment will be given by $(H_\infty + dH_\infty)$. The porosity variation of the suspension AB in Figure 9(a) is identical to that of the suspension A^-B^- in Figure 9(b). Consequently, the total solids volume $(\omega_o + d\omega_o)$ in the sediment A^-C^- can be represented by :

$$\omega_o + d\omega_o = \omega_o + dH_\infty(1-\epsilon) \tag{15}$$

where H_∞ = final equilibrium height of sediment, (m)

ω_o = total volume of dry solids per unit cross-sectional area of tube or cylinder, (m^3/m^2)

Solving for ϵ in equation (15) :

$$\epsilon = 1 - \frac{d\omega_o}{dH_\infty} \tag{16}$$

ω_o is related to the solids compressive pressure P_s by the relation :

$$P_s = (\rho_s - \rho_l) g \omega_o \tag{17}$$

where g = constant of gravitational acceleration (m/s^2)

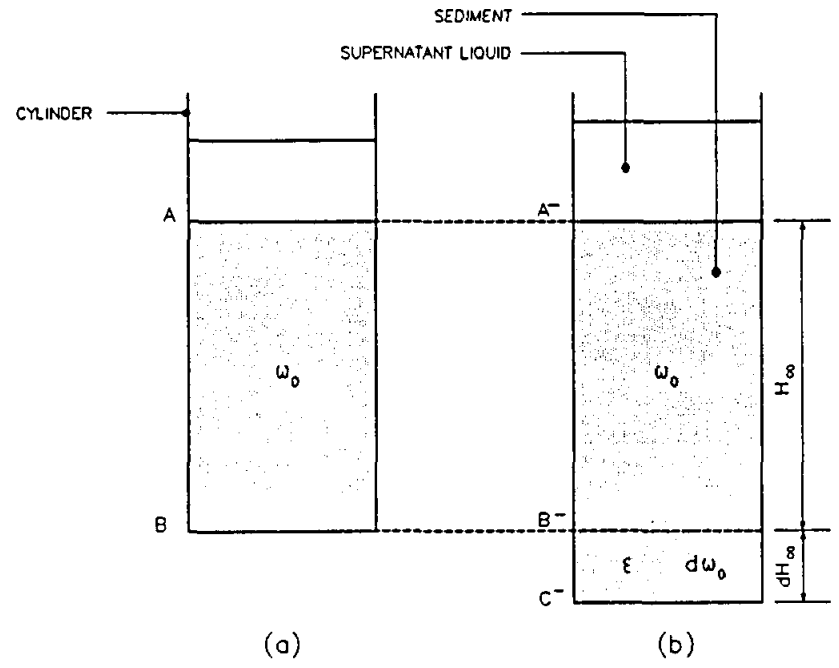

FIGURE 9 **Schematic Diagram Showing the Relationship Between Height of Sediment and Volume of Dry Solids per Unit Area**

Shirato et al. (1983) found that on the basis of experimental data, H_∞ could be represented in terms of ω_0 by the following equation :

$$H_\infty = a\omega_0^b \tag{18}$$

where a = empirical constant in equation (18)

b = empirical constant in equation (18)

Substituting equation (18) into equation (16) and eliminating ω_0 by means of equation (17), one obtains equation (19) :

$$(1-\epsilon) = BP_s^\beta \tag{19}$$

where

$$B = \frac{1}{ab[(\rho_s-\rho_l)g]^{(1-b)}} \tag{20}$$

and

$$\beta = 1-b \tag{21}$$

The values of empirical constants a and b may be obtained from a linear regression using the experimental results of log H_∞ and log ω_o. From equation (18) :

$$\log H_\infty = \log a + b \log \omega_o \qquad (22)$$

The values of B and β are calculated from equations (20) and (21), respectively. The relationship between porosity and solids compressive pressure can be calculated from equation (9).

b Determination of Permeability

The following technique for determining permeability at low solids compressive pressures, was also developed by Shirato et al. (1983).

Michaels and Bolger (1962) investigated the sedimentation behaviour of flocculated suspensions of kaolin. For their sedimentation model they assumed that for flocculated suspensions, the basic flow units or settling entities are small clusters of particles or flocs. For gravity settling the flocs group into clusters of flocs called particle or floc aggregates. Michaels and Bolger (1962) found that the floc aggregates determine the sedimentation behaviour of flocculated suspensions. Shirato et al. (1983) confirmed the results of Michaels and Bolger (1962).

By using zinc oxide, Mitsukuri Gairome clay and ferric oxide slurries, they showed that sedimentation behaviour may be classified into three general regions according to the initial porosity of a suspension, ϵ_{in}, as shown in Figure 10.

In the dilute concentration region, $\epsilon_{in} > \epsilon_L$, free or hindered settling of individual particles or aggregates of particles may occur. In the intermediate concentration region, $\epsilon_{if} < \epsilon_{in} < \epsilon_L$, sedimentation behaviour becomes unstable owing to partial collapse of particle aggregates. In the higher concentration region, $\epsilon_{in} < \epsilon_{if}$, the supernatant liquid/sediment interface subsides slowly due to slow *consolidation* or *compression* of the sediment. In order to describe the sedimentation behaviour in the dilute concentration region, Michaels and Bolger (1962) modified an equation which Richardson and Zaki (1954) developed for the hindered settling of uniform, spherical particles. According to the modified equation, for dilute suspensions ($\epsilon_{in} > \epsilon_L$) of small clusters or aggregates of particles, the initial settling velocity of the surface of the sediment, v_o, can be related to the initial porosity, ϵ_{in}, of the original suspension :

$$v_o^{\frac{1}{4.65}} = \left\{ \frac{g d_f^2 (\rho_s - \rho_l)}{18 \mu_f (1 - \epsilon_{if})^{3.65}} \right\}^{\frac{1}{4.65}} (\epsilon_{in} - \epsilon_{if}) \qquad (23)$$

where d_f = mean diameter of particle aggregates (m)

v_o = initial settling velocity of surface of sediment (m/s)

ϵ_{if} = internal porosity of particle aggregates (-)

ϵ_{in} = initial porosity of suspension (-)

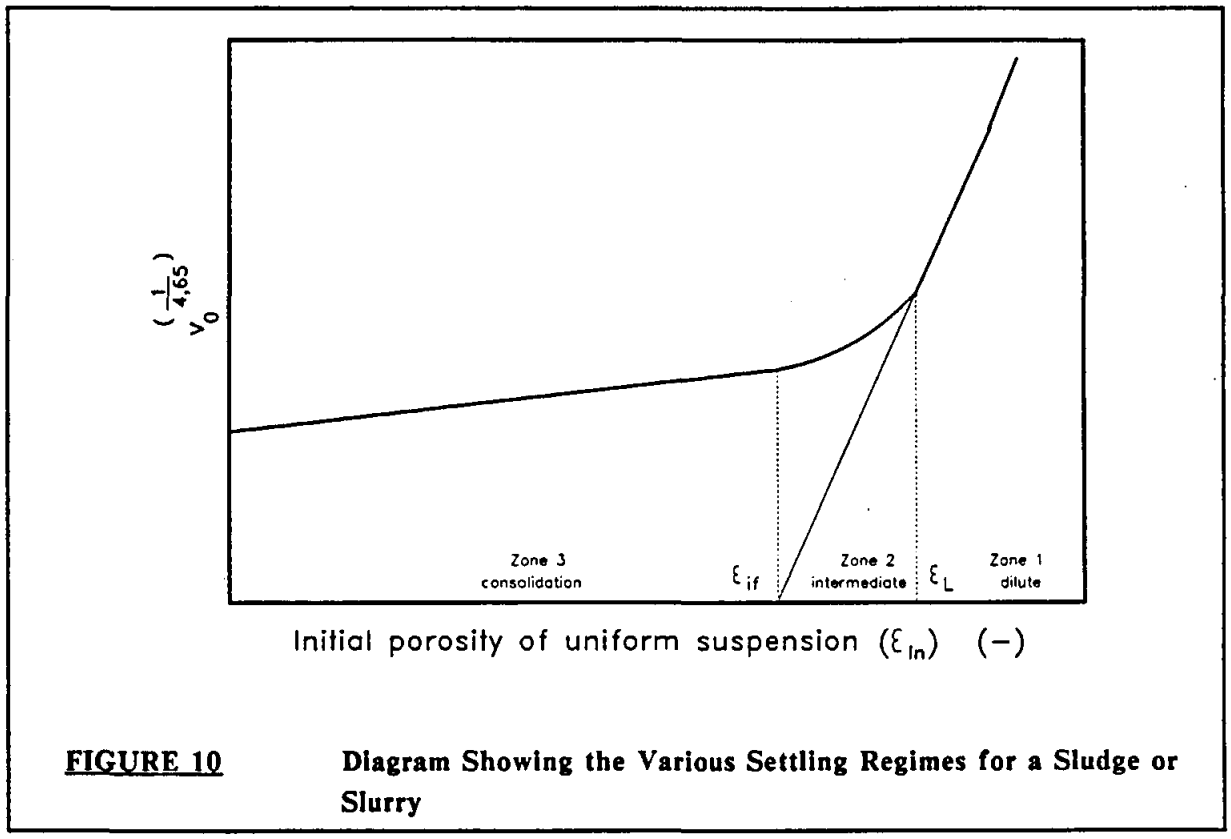

FIGURE 10 **Diagram Showing the Various Settling Regimes for a Sludge or Slurry**

As shown in Figure 10, a straight line is obtained in the dilute region ($\epsilon_{in} > \epsilon_L$) in accordance with equation (23).

The above techniques for measuring porosity and permeability at low solids compressive pressures are only valid for the concentration region, $\epsilon_{in} < \epsilon_{if}$, where sedimentation occurs due to *consolidation* of the sediment (Shirato et al., 1983).

For batch sedimentation of a concentrated suspension inside a cylinder, the liquid pressure, P_L, and the solids compressive pressure, P_s, increase towards the bottom of the cylinder. When a thin layer of the suspension settles due to consolidation, liquid has to flow through the thin layer due to the liquid pressure gradient across the layer as shown in Figure 11. The liquid pressure gradient across an element is caused by the weight of the particles lying above the element.

The D'Arcy equation may be used to describe the liquid flow through the thin layer :

$$u_l = -\frac{K}{\mu}\frac{\partial P_l}{\partial y} \qquad \textit{from (1)}$$

where u_l = apparent liquid velocity relative to solids (m/s)

y = distance measured from bottom of cylinder (m)

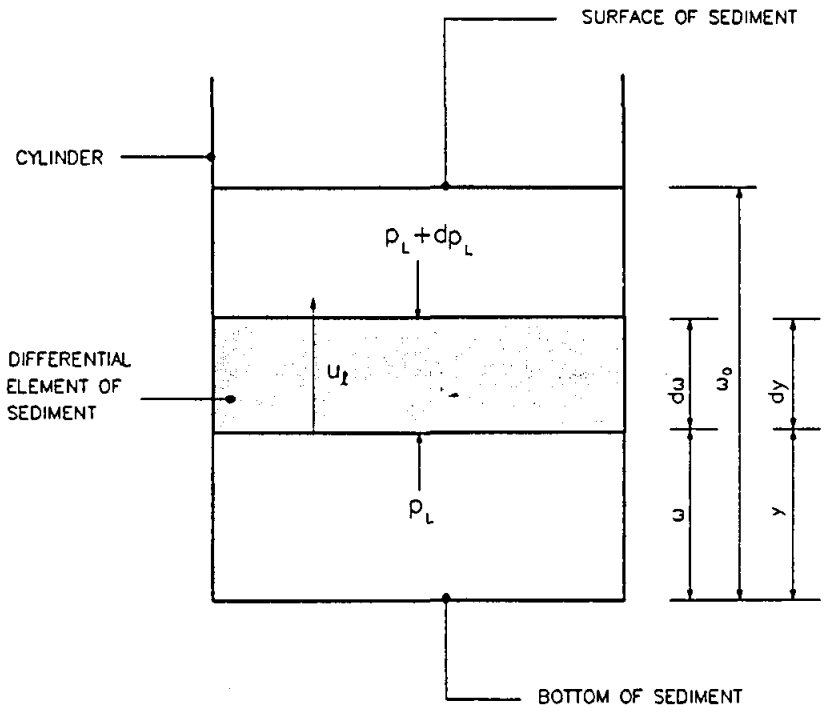

FIGURE 11 **Schematic Diagram Showing Up-flow of Liquid Due to Liquid Pressure Gradient in "Consolidation" Settling Regime**

But

$$d\omega = (1-\epsilon)dy \qquad (24)$$

where ω = volume of dry solids per unit cross-sectional area of tube or cylinder measured from bottom of tube or cylinder, (m^3/m^2)

Therefore the D'Arcy equation may be written in terms of ω, as follows :

$$u_l = -\frac{K(1-\epsilon)}{\mu_l}\frac{\partial P_l}{\partial \omega} \qquad (25)$$

The forces acting on a differential element, $d\omega$, are shown in Figure 12. The following equation may be derived from Newton's second law of motion (assuming acceleration and inertial effects to be negligible) :

$$\frac{\partial P_l}{\partial \omega} + \frac{\partial P_s}{\partial \omega} = -(\rho_s - \rho_l)g \qquad (26)$$

Wall friction is assumed to be negligible.

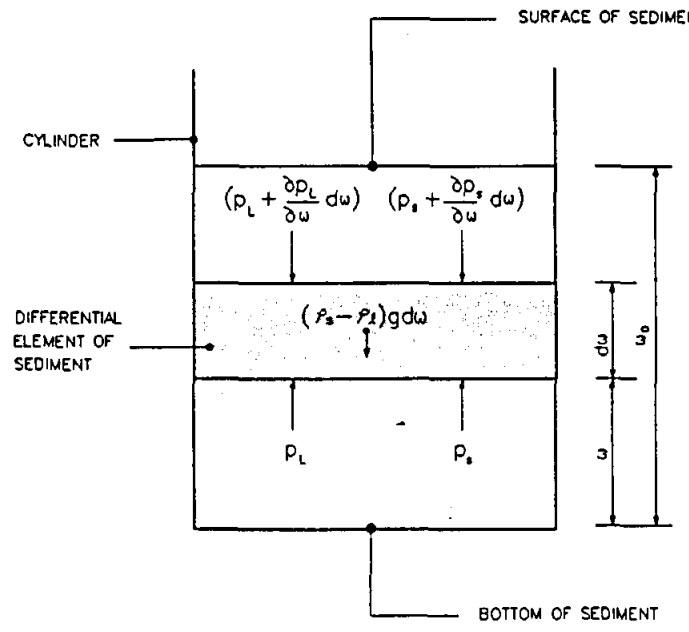

FIGURE 12 **Forces Exerted on a Differential Element $d\omega$, in the "Consolidation" Settling Regime**

Since the solids compressive pressure, P_s, can be assumed to be constant throughout the height of the cylinder at the beginning of a settling test when the suspension is uniform (Shirato et al., 1983), the initial liquid pressure gradient can be obtained from equation (26).

$$\left(\frac{\partial P_l}{\partial \omega}\right)_{t=0} = -(\rho_s - \rho_l)g \qquad (27)$$

At time, $t = 0$, u_l in equation (25) can be considered as a constant which is equal to the initial settling velocity of the sediment surface, v_o. Combining equations (25) and (27) :

$$K = \frac{v_o \mu_f}{(\rho_s - \rho_l)(1 - \epsilon_{in})g} \qquad (28)$$

But from equation (2) :

$$K = \frac{1}{\rho_s \alpha (1 - \epsilon_{in})} \tag{29}$$

Therefore,

$$\alpha = \frac{(\rho_s - \rho_l) g}{\mu_l \rho_s v_o} \tag{30}$$

On the assumption that the initial settling velocity depends only on the initial concentration of a suspension, equations (28) and (30) in conjunction with batch sedimentation data permit the calculation of permeability and specific filtration resistance, respectively.

Shirato et al. (1983) obtained the initial settling velocity, v_o, of a suspension by plotting (H/H_i) versus (t/H_i) for different initial heights, H_i, in a cylinder. H is the height of the interface between the supernatant liquid and the sediment at time, t, while H_i is the initial height of the uniform suspension in the cylinder. For the experimental results of Shirato et al. (1983), the initial settling velocity of a suspension, v_o, was not affected by the initial height of the uniform suspension in a cylinder, H_i.

3.2.2.2 Apparatus and procedure

No *standardised* apparatus has been specified for the settling tests. The actual apparatus and procedure adopted in the tests on the waterworks clarifier sludge are summarised below.

a Porosity

Various quantities of homogenized sludge were introduced into eight perspex cylinders with an internal diameter of 60 mm. The initial heights of the sludge in the cylinders were in the range of approximately 0,05 m to approximately 1,5 m. The initial solids concentration of the sludge was sufficiently high so as to be in the region where settling occurs due to compaction or consolidation from the beginning of the experiment.

The heights of the interfaces between the sediment and supernatant liquid in the cylinders were measured at regular intervals. It was found that there was no further compaction or consolidation after approximately 2 weeks of standing.

The final equilibrium heights were recorded. The results were then analysed according to the model proposed by Shirato et al. (1983) which was described in Section 3.2.2.1(a)

b Permeability

Various quantities of homogenized sludge were introduced into 4 polypropylene measuring cylinders, each with a capacity of 1 ℓ and an internal diameter of 50 mm. The initial solids concentration of the sludge was sufficiently high for sedimentation to occur by compaction or consolidation from the beginning of the experiment.

The initial heights of the sludge were 159 mm; 239 mm; 318 mm and 397 mm for all initial solids concentrations which were tested. The heights of the interfaces between the sediment and the supernatant liquid were measured at regular time intervals for various initial solids concentrations.

The results were analysed according to the model proposed by Shirato et al. (1983), which was described in Section 3.2.2.1(b).

3.2.3 Centrifuge Method

Shirato et al. (1983) found good agreement between the compression-permeability results from a C-P cell (at high solids compressive pressure) and those obtained using the settling technique (at low solids compressive pressure). However, Murase et al. (1989) did not find good correlation between the porosity results using the settling technique and those obtained from a C-P cell and a new centrifuge technique. They ascribed this to friction between the suspension and the inner wall of the cylinder during batch settling. Murase et al. (1989) gave results of $(1-\epsilon)$ versus P_s for zinc oxide and ferric oxide slurries for all three techniques. The results for the settling tests were in the P_s range, $30\,\text{Pa} < P_s < 1000\,\text{Pa}$, for the centrifuge tests the results were in the P_s range, $10^3\,\text{Pa} < P_s < 10^5\,\text{Pa}$, and for the C-P cell tests the results were in the P_s range, $10^5\,\text{Pa} < P_s < 10^7\,\text{Pa}$. They recommended the centrifuge technique for determining the variation of porosity with solids compressive pressure in the intermediate P_s range.

3.2.3.1 Theory

Figure 13 shows a suspension which has reached an equilibrium thickness in a rotating centrifuge tube. The forces acting on a thin element of sediment, Δr_c, are shown in Figure 13. The following equation may be derived from Newton's second law of motion (at equilibrium) :

$$F_c(r+\Delta r) - F_c(r) = (\rho_s - \rho_l)(1-\epsilon)(\pi r_t^2 \Delta r_c) r_c \Omega^2 \qquad (31)$$

where F_c = solids compressive force (N)

r_c = distance from centre of centrifuge (m)

r_t = radius of centrifuge tube (m)

Δr_c = thickness of differential element of sediment (m)

Ω = angular velocity (rad/s)

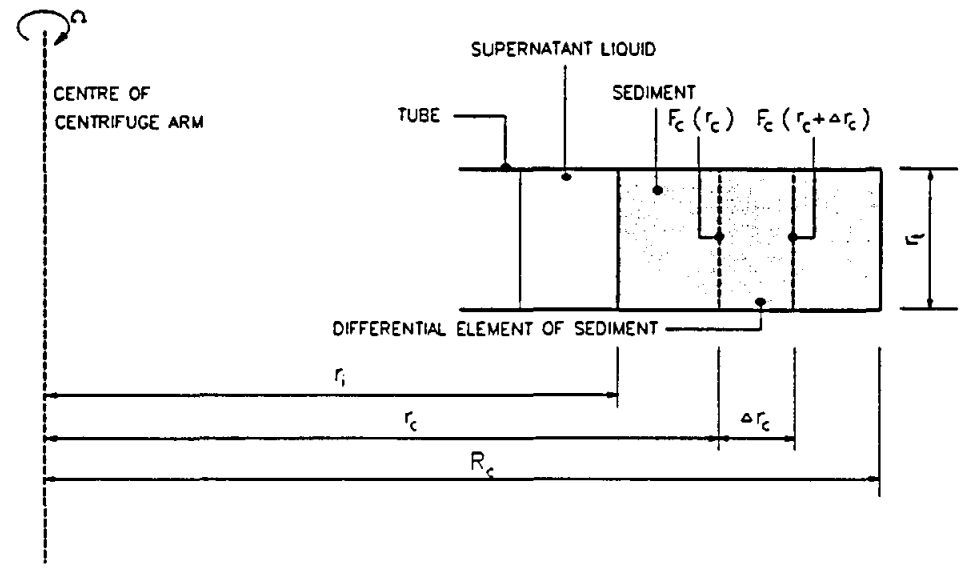

FIGURE 13 **Forces Acting on Differential Element of Sediment in Centrifuge Tube**

In the limit, as $\Delta r_c \rightarrow 0$, equation (31) becomes :

$$\frac{dP_s}{dr_c} = (\rho_s - \rho_l)(1-\epsilon) r_c \Omega^2 \tag{32}$$

Integration of equation (32) with respect to r_c yields the following equation for the solids compressive pressure at the bottom of the tube, $P_s(R_c)$:

$$P_s(R_c) = (\rho_s - \rho_l)\Omega^2 \int_{r_l}^{R_c} (1-\epsilon) r_c dr_c \tag{33}$$

where R_c = distance between centre of centrifuge and bottom of centrifuge tube (m)

r_l = distance from centre of centrifuge to surface of sediment (m)

If $R_c \gg (R_c - r_l)$, the variable r_c in equation (33) can be approximated by $(R_c + r_l)/2$. Therefore

$$P_s(R_c) = (\rho_s - \rho_l)\Omega^2 \frac{(R_c + r_l)}{2} \int_{r_l}^{R_c} (1-\epsilon) dr_c$$

$$= (\rho_s - \rho_l)\Omega^2 \left(\frac{R_c + r_l}{2}\right) \omega_o \tag{34}$$

where ω_o = total volume of dry solids per unit cross-sectional area of tube or cylinder (m^3/m^2)

As noted in Section 3.1, set of equations (9) has generally been used to model the variation of porosity with solids compressive pressure, P_s:

$$(1-\epsilon) = BP_s^{\beta} \qquad P_s \geq P_{si}$$

$$(1-\epsilon_i) = BP_{si}^{\beta} \qquad P_s \leq P_{si} \tag{9}$$

Combining equations (32) and (9) and integrating equation (32) over the entire sediment layer one obtains :

$$\int_o^{P_{si}} \frac{dP_s}{BP_{si}^{\beta}} + \int_{P_{si}}^{P_s(R_c)} \frac{dP_s}{BP_s^{\beta}} = (\rho_s - \rho_l)\Omega^2 \int_{r_i}^{R_c} r_c dr_c \tag{35}$$

Therefore,

$$\frac{P_{si}^{(1-\beta)}}{B} + \frac{P_s(R_c)^{(1-\beta)} - P_{si}^{(1-\beta)}}{B(1-\beta)} = (\rho_s - \rho_l)\Omega^2 \frac{(R_c + r_i)}{2}(R_c - r_i) \tag{36}$$

Combining equations (34) and (36) yields the following equation :

$$R_c - r_i = \frac{\omega_o^{(1-\beta)}}{B(1-\beta)} \left\{(\rho_s - \rho_l)\frac{(R_c + r_i)}{2}\Omega^2\right\}^{-\beta} - \frac{\beta P_{si}^{(1-\beta)}}{B(1-\beta)} \left\{(\rho_s - \rho_l)\frac{(R_c + r_i)}{2}\Omega^2\right\}^{-1} \tag{37}$$

Murase et al. (1989) found that for their results the second term on the right hand side of equation (37) was negligible. They obtained a good linear correlation when they plotted log $(R_c - r_i)$ versus log $\left\{(\rho_s - \rho_l)\frac{(R_c+r_i)}{2}\Omega^2\right\}$. From such a plot and by ignoring the second term of equation (37), the values of the constants B and β can be determined. The porosity versus P_s relationship can then be obtained from set of equations (9).

3.2.3.2 Apparatus and Procedure

Similar to the settling tests, no standardised apparatus exists for the centrifuge tests. The actual apparatus used and procedure followed is described below.

Equal amounts of homogenized sludge were introduced into four flat-bottomed centrifuge tubes. The details of the tubes are presented in Rencken (1992). The tubes were placed in their holders in the centrifuge and were then spun at a fixed speed for 1 hour. Previous experiments had shown that the thickness of the sediments in the tubes did not change significantly after rotating for more than 1 hour.

The thickness of the sediments in the tubes was then measured. The tubes were then again placed in their holders in the centrifuge and were then spun at a higher rotational speed.

The rotational speed was varied in the range 500 r.p.m. (52,36 rad/s) to 4 000 r.p.m. (418,88 rad/s).

3.3 RESULTS

The methods discussed in Section 3.2 to determine CPV data were applied to characterise a waterworks clarifier sludge obtained from Umgeni Water's H D Hill Water Works. The objectives were :

(i) to determine the validity of methods when applied to the waterworks sludge, i.e. to determine whether the methods produce meaningful trends that were consistent with the theories of the methods.

(ii) to determine the repeatibility of the methods. This was done by performing two sets of tests for each method.

(iii) to determine the applicability of the correlative models stated in Section 3.1, by ascertaining whether the experimental results could be correlated in terms of the proposed models.

3.3.1 C-P Cell Experiments

Two sets of tests, A.1 and A.2, were performed on the waterworks sludge. Plots of permeability versus solids compressive pressure and solids volume fraction $(1 - \epsilon)$ versus solids compressive pressure for the two tests are shown in Figures 14 and 15 respectively.

Linear regressions using the permeability versus solids compressive pressure data for tests A.1 and A.2 yielded values for F and δ (see set of equations (8)) as shown in Table 1.

Linear regressions using the solids volume fraction $(1 - \epsilon)$ versus solids compressive pressure data for tests A.1 and A.2 yielded values for B and β (see set of equations (9)) as shown in Table 2.

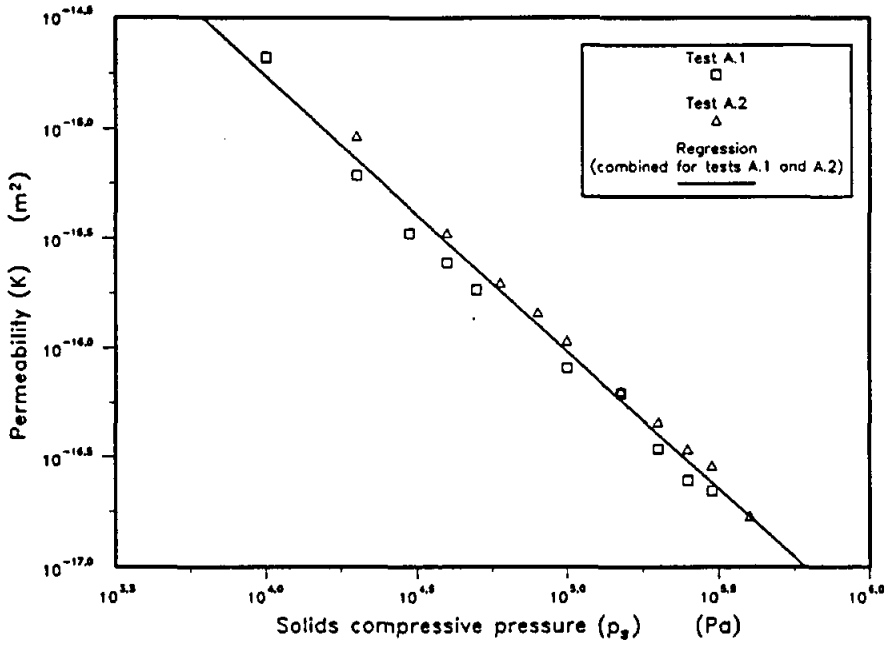

FIGURE 14 **Graph of Permeability versus Solids Compressive Pressure for the C-P Cell Experiments -**

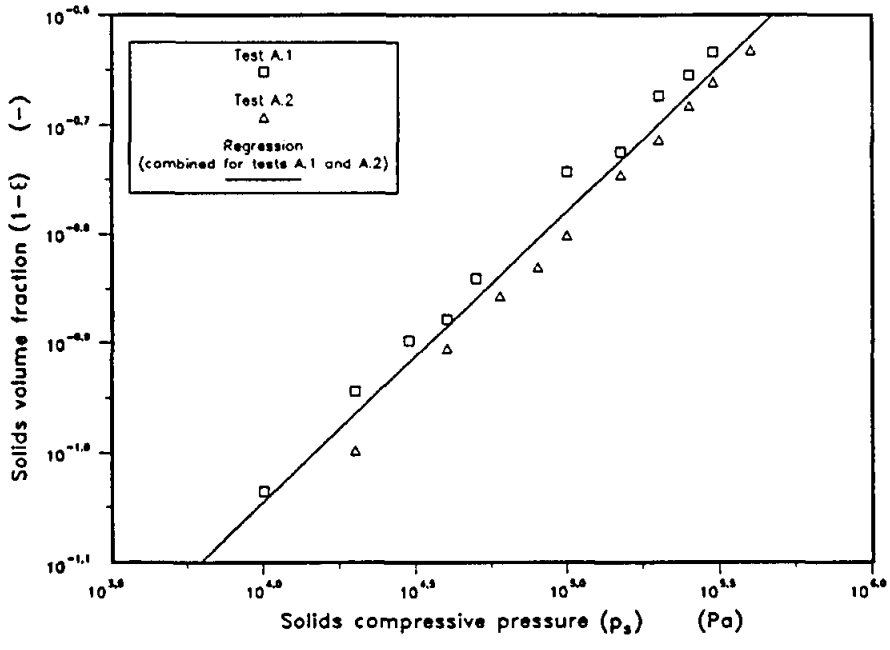

FIGURE 15 **Graph of Solids Volume Fraction versus Solids Compressive Pressure for the C-P Cell Experiments**

TABLE 1
Linear Regression Values for F , δ and Correlation Coefficient (r_r^2) for C-P Cell Test A.1, Test A.2 and Tests A.1 and A.2 *Combined*

	Test A.1	Test A.2	Tests A.1 and A.2 *Combined*
F	2,129 x 10^{-10}	2,922 x 10^{-10}	1,779 x 10^{-10}
δ	1,281	1,286	1,254
r_r^2	0,991	0,998	0,985

TABLE 2
Linear Regression Values for B , β and Correlation Coefficient (r_r^2) for C-P Cell Test A.1, Test A.2 and Tests A.1 and A.2 *Combined*

	Test A.1	Test A.2	Tests A.1 and A.2 *Combined*
B	0,00771	0,00621	0,00785
β	0,271	0,282	0,265
r_r^2	0,996	0,999	0,974

It is seen that the results from the C-P cell follow the form indicated by set of equations (9). However, while the results for each individual set yield good correlation coefficients, the combined results have a greater scatter and hence a lower correlation coefficient. From Figure 15, it seems that while the results for each set lie along straight lines, the lines are somewhat offset from each other. This is an indication of the attainable repeatibility for C-P cell experiments. Accordingly, in employing the results depicted in Figure 15, confidence levels based on the scatter between the sets must be established. This is discussed further in Section 3.3.4.3.

For specific filtration resistance the values of C and n in set of equations (10) (for *combined* tests A.1 and A.2) were calculated :

$$C = 3{,}008 \times 10^{8}$$

$$n = 0{,}989$$

3.3.2 Settling Experiments

3.3.2.1 Determination of Porosity

Two settling tests (tests B.1 and B.2) were performed to determine the relationship between porosity and solids compressive pressure at low solids compressive pressure. A plot of H_∞ versus ω_o for both tests is shown in Figure 16. Linear regressions using the H_∞ versus ω_o data for tests B.1 and B.2 yielded values for a and b (see equation (18)) as shown in Table 3.

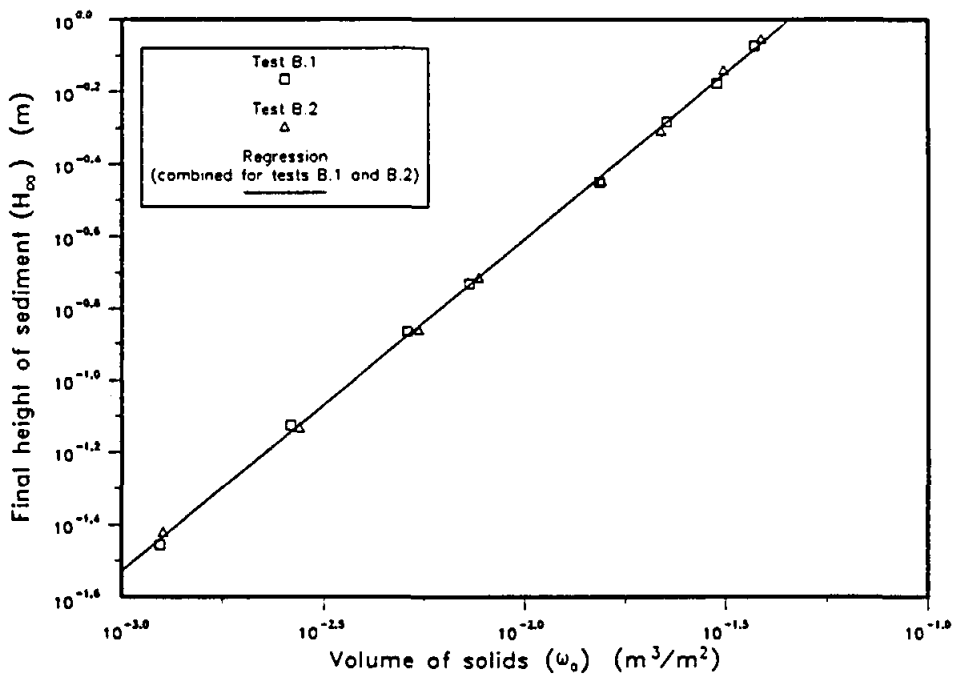

FIGURE 16 **Graph of Final Height of Sediment versus Volume of Solids for the Settling Experiments**

TABLE 3
Linear Regression Values for a, b and Correlation Coefficient (r_r^2) for Settling Test B.1, Test B.2 and Tests B.1 and B.2 *Combined*

	Test B.1	Test B.2	Tests B.1 and B.2 *Combined*
a	17,108	17,391	17,248
b	0,9201	0,9235	0,9218
r_r^2	0,999	0,999	0,999

Here it is observed that repeatibility between the sets is good, obviating the necessity to establish confidence intervals for the regressed equations.

The density of the solids in the sludge was experimentally determined as 2380,1 kg/m^3. Taking the density of water as 997,69 kg/m^3 (at 22,5 °C; Perry, 1973), the value for B for the *combined* regression data may be calculated from equation (20) for the values of a and b for the *combined* H_∞ versus ω_0 data.

$$B = \frac{1}{ab[(\rho_s - \rho_l)g]^{(1-b)}}$$

$$= \frac{1}{(17,248)(0,9218)[(2380.1 - 997,69)(9.81)]^{(1-0.9218)}}$$

$$= 0,0299$$

From equation (21) :

$$\beta = 1 - b$$

$$= 1 - 0,9218$$

$$= 0,0782$$

From set of equations (9) :

$$1 - \epsilon = BP_s^{\beta}$$

$$= 0,0299\, P_s^{0,0782} \qquad \left(\begin{array}{c} \textit{for combined regression data} \\ \textit{for tests B.1 and B.2} \end{array}\right)$$

The values of B and β for test B.1, test B.2 and tests B.1 and B.2 *combined* are shown in Table 4 :

TABLE 4
Values for B and β for Settling Test B.1, Test B.2 and Tests B.1 and B.2 *Combined*

	Test B.1	Test B.2	Tests B.1 and B.2 *Combined*
B	0,0297	0,0301	0,0299
β	0,0799	0,0765	0,0782

A plot of solids volume fraction $(1 - \epsilon)$ versus solids compressive pressure for the settling experiments, is shown in Figure 17. The solids compressive pressure range for these experiments was, 16,9 Pa $\leq P_s \leq$ 525.6 Pa .

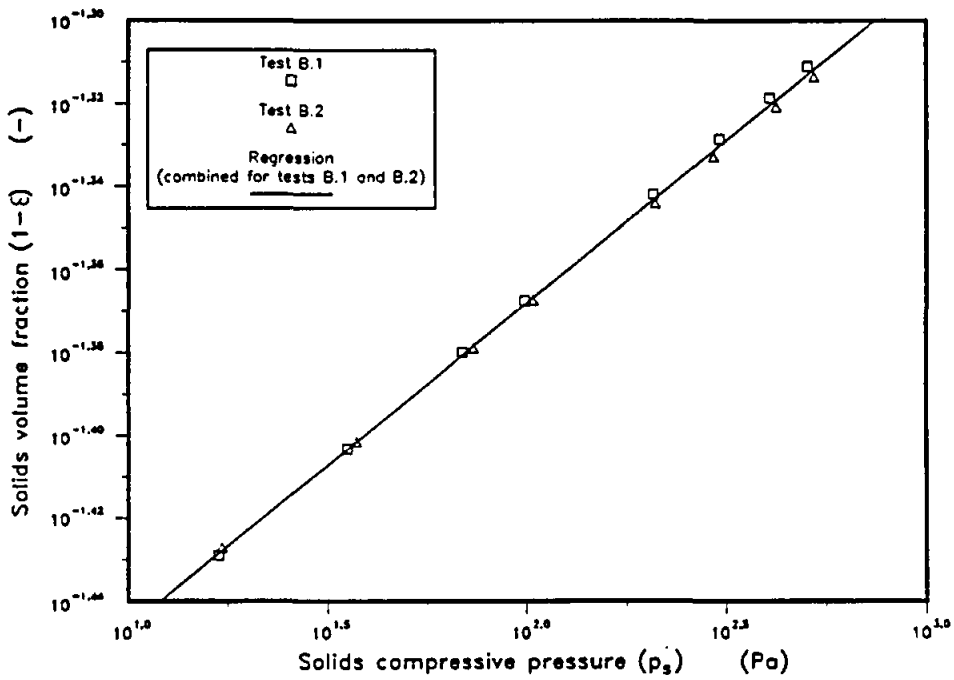

FIGURE 17 **Graph of Solids Volume Fraction versus Solids Compressive Pressure for the Settling Experiments**

3.3.2.2 Determination of Permeability

The results of the settling tests to determine the variation of permeability with solids compressive pressure at low solids compressive pressures were plotted in the form of Figure 10. This is shown in Figure 18.

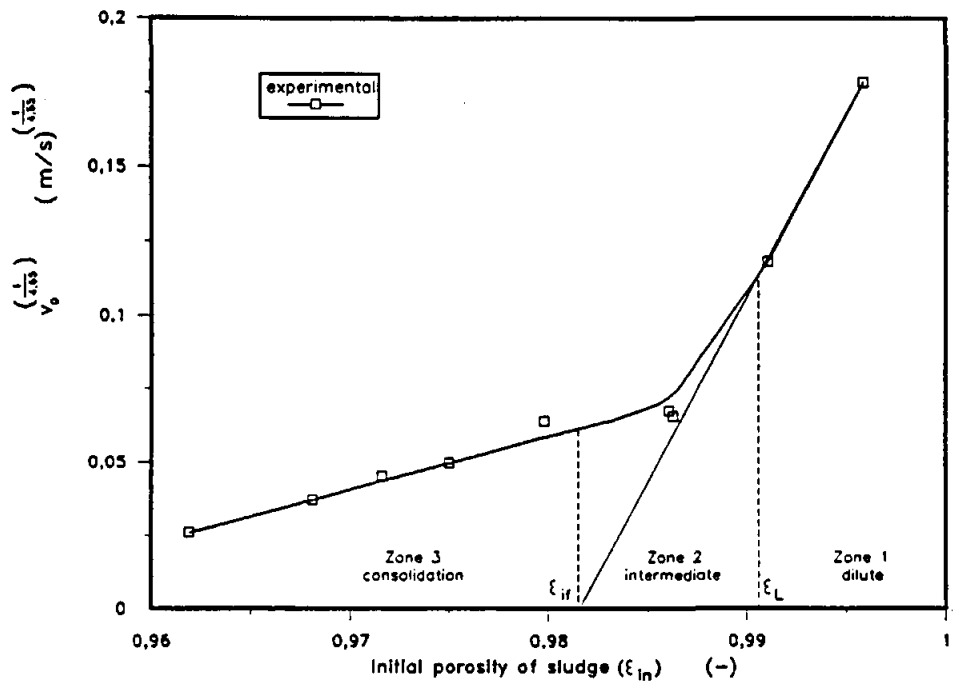

FIGURE 18 **Graph of $v_o^{\left(\frac{1}{4.65}\right)}$ versus Initial Porosity of Sludge (ϵ_{in}) for Settling Tests**

From Figure 18, it was determined that for the sludge :

ϵ_L = 0.991

ϵ_{if} = 0.982 (see Figure 10)

A plot of permeability versus solids compressive pressure is shown in Figure 19. The solids compressive pressure range for these experiments was, 0.0065 Pa $\leq P_s \leq$ 22.55 Pa .

A linear regression using the permeability versus solids compressive pressure data yielded the following values for F and δ (see set of equations (8)) in the solids compressive pressure range which was investigated :

$F = 6.621 \times 10^{-13}$

δ = 0.575

The correlation coefficient, r_r^2, for the regression was 0,977.

The values of C and n for specific filtration resistance (see set of equations (10)) were calculated for the settling experiments :

$$C = 2.122 \times 10^{10}$$

$$n = 0.497$$

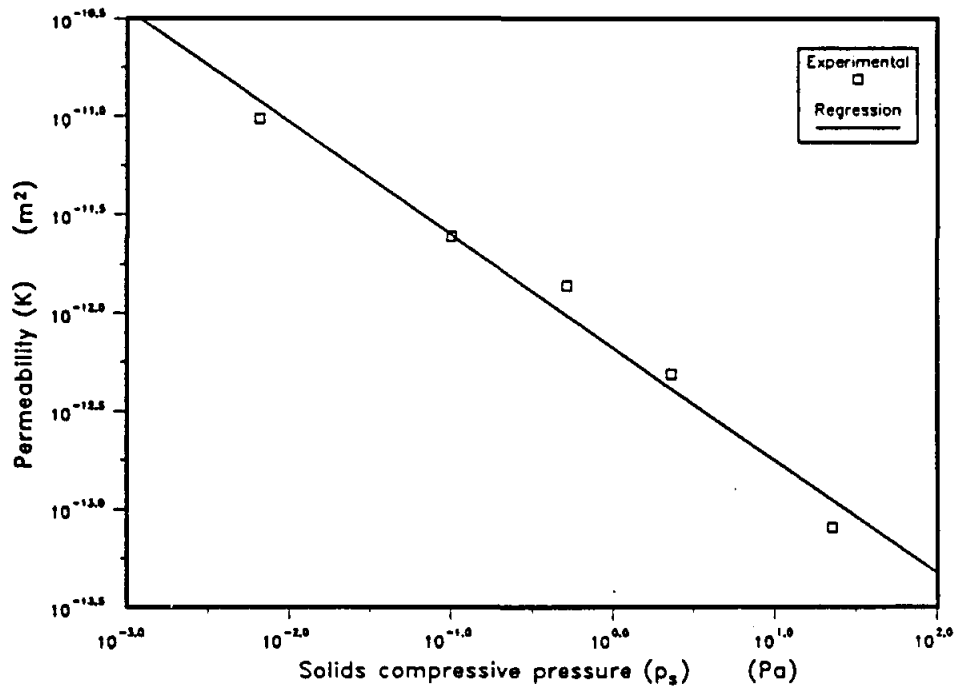

FIGURE 19 **Graph of Permeability (K) versus Solids Compressive Pressure (P_s) for the Settling Experiments**

3.3.3 Centrifuge Experiments

Two sets of centrifuge tests were performed, tests C.1 and C.2. As stated in section 3.2.3, Murase et al. (1989) found that the second term on the right hand side of equation (37) could be ignored. This gives the following equation:

$$(R_c - r_i) = \frac{\omega_o^{(1-\beta)}}{B(1-\beta)} \left\{ (\rho_s - \rho_l) \frac{(R_c + r_i)}{2} \Omega^2 \right\}^{-\beta} \qquad (38)$$

By plotting $(R_c - r_i)$ versus $\left\{ (\rho_s - \rho_l) \frac{(R_c + r_i)}{2} \Omega^2 \right\}$ on a log scale, a straight line should be obtained.

A graph of $(R_c - r_i)$ versus $\left\{ (\rho_s - \rho_l) \frac{(R_c + r_i)}{2} \Omega^2 \right\}$, for the tests C.1 and C.2 is shown in Figure 20.

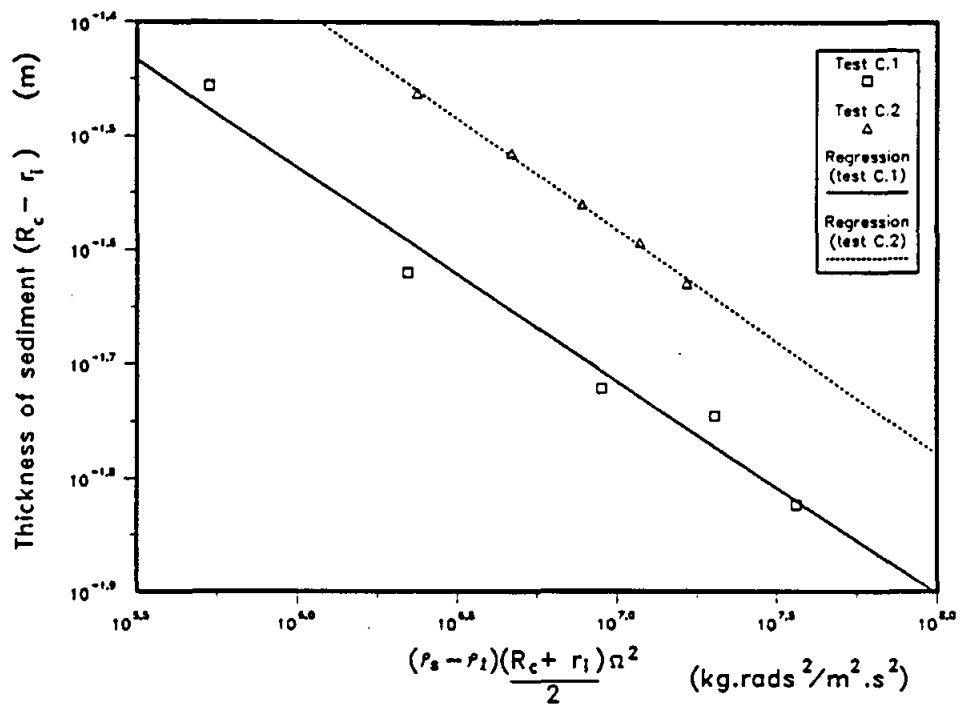

FIGURE 20 **Graph of Thickness of Sediment $(R_c - r_i)$ versus $\left\{(\rho_s - \rho_l)\left(\frac{R_c + r_i}{2}\right)\Omega^2\right\}$ for the Centrifuge Experiments**

The values for B and β, which were obtained from linear regressions using the data for tests C.1 and C.2, are shown in Table 5 :

TABLE 5
Linear Regression Values for B, β and Correlation Coefficient (r_r^2) for Centrifuge Test C.1, Test C.2 and Tests C.1 and C.2 *Combined*

	Test C.1	Test C.2	Tests C.1 and C.2 *Combined*
B	0,0177	0,0175	0,0169
β	0,187	0,196	0,196
r_r^2	0,973	0,998	0,981

A plot of solids volume fraction (1 - ϵ) versus solids compressive pressure for the centrifuge tests is shown in Figure 21.

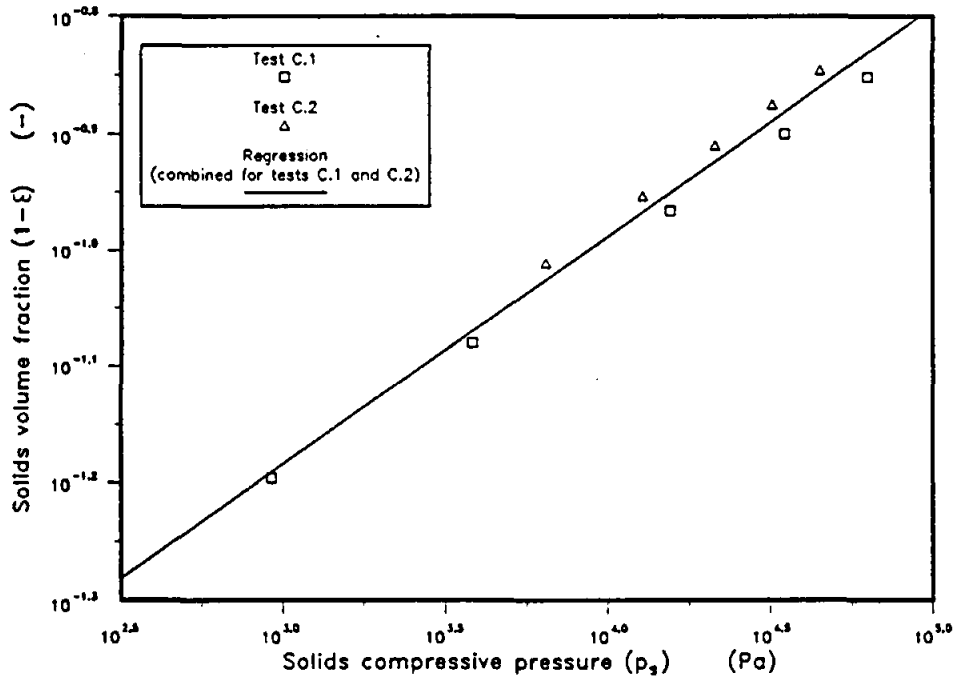

FIGURE 21 **Graph of Solids Volume Fraction (1 - ϵ) versus Solids Compressive Pressure (P_s) for the Centrifuge Experiments**

3.3.4 Fitting of Porosity and Permeability Data to Standard Equations

3.3.4.1 Permeability Data

A graph of permeability versus solids compressive pressure for the settling tests and the two C-P cell tests is shown in Figure 22. The regression lines for the settling and *combined* C-P cell data are also shown. From Figure 22 it is evident that the slopes of the regression lines are different. The two lines intersect at a solids compressive pressure of 3781,7 Pa.

The following equations are based on the linear regression results of the *combined* C-P cell and settling data, as shown in sections 3.3.1 and 3.3.2.2, respectively :

$$K = 6.621 \times 10^{-13} P_s^{-0.575} \qquad P_s \leq 3781.7\,\text{Pa}$$

$$K = 1.779 \times 10^{-10} P_s^{-1.254} \qquad P_s \geq 3781.7\,\text{Pa} \qquad (39)$$

From set of equations (39), $K \to \infty$ as $P_s \to 0$. In order to prevent this it was assumed that below the solids compressive pressure, P_{sf}, the permeability is constant. Solids compressive pressure, P_{sf}, was defined as follows from set of equations (9) :

$$P_{sf} = \left(\frac{1-\epsilon_f}{B}\right)^{\frac{1}{k}} \tag{40}$$

where P_{sf} = solids compressive pressure corresponding to porosity of feed sludge, (Pa)

ϵ_f = porosity of feed sludge, (-)

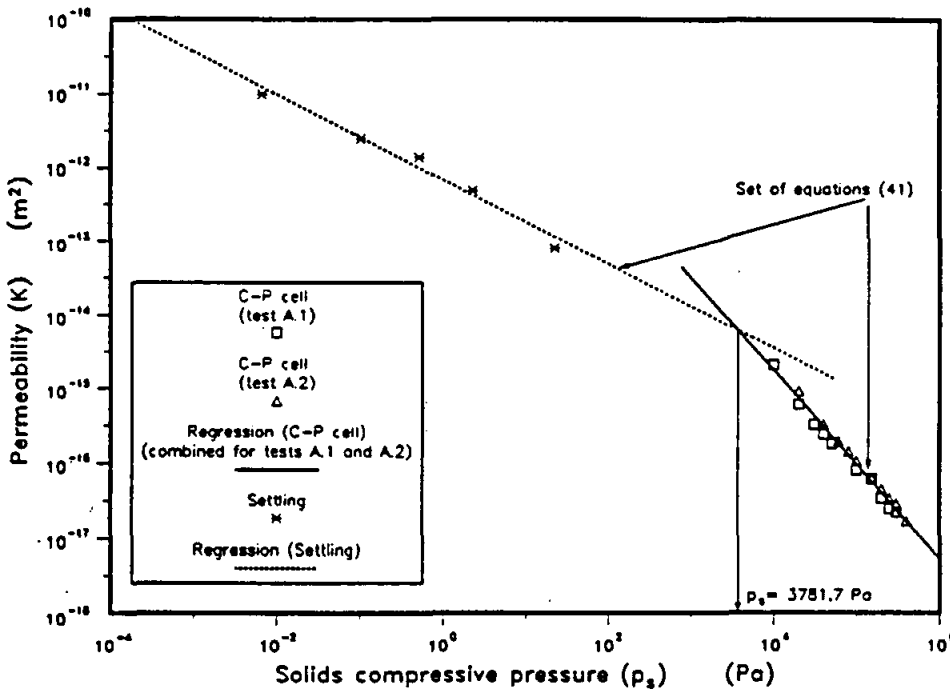

FIGURE 22 **Graph of Permeability (K) versus Solids Compressive Pressure (P_s) for the C-P Cell and Settling Experiments Showing the Basis for Set of Equations (41)**

The equations which were used to describe the permeability versus solids compressive pressure relationship for the clarifier sludge, were therefore :

$$\begin{aligned} K &= 6.621 \times 10^{-13} P_{s,f}^{-0.575} && 0 \leq P_s \leq P_{s,f} \\ K &= 6.621 \times 10^{-13} P_s^{-0.575} && P_{s,f} \leq P_s \leq 3781.7\ \text{Pa} \\ K &= 1.779 \times 10^{-10} P_s^{-1.254} && P_s \geq 3781.7\ \text{Pa} \end{aligned} \qquad (41)$$

Unless the solids concentration of the feed sludge is very high, the value of $P_{s,f}$ will be small. For a feed sludge solids concentration of 49 g/ℓ, as was used in this study, and using the regression results of the settling tests :

$$\begin{aligned} P_{s,f} &= \left(\frac{1 - 0.9794}{0.0299}\right)^{\frac{1}{0.0762}} \\ &= 0.0085\ \text{Pa} \end{aligned}$$

The set of equations (41) is similar to the set of equations (8) which was proposed by Tiller and Cooper (1962).

Murase et al. (1989) also reported different slopes for settling data and C-P cell data. They ascribed this to network formation between aggregates of particles in the concentration range where settling occurs due to consolidation or compaction. According to them the network formation leads to significant friction between particles and the inner wall of the cylinder and therefore to erroneous results. However, a good fit between experimental results and the planar and internal cylindrical filtration models, using set of equations (41), was obtained.

The resistance of the cake was very high. The average specific filtration resistance (for planar filtration) was calculated to be 1,351 x 10^{13} m/kg for an applied filtration pressure of 300 kPa.

3.3.4.2 Porosity Data

A graph of $(1 - \epsilon)$ versus P_s for the settling data, centrifuge data and the C-P cell data is shown in Figure 23. It is evident that the three sets of data for the three different methods all have significantly different slopes. The agreement between the C-P cell data and the centrifuge data is not nearly as good as that reported by Murase et al. (1989). A linear regression using the *combined* centrifuge and C-P cell data yielded the following results :

$$B = 0.0125$$

$$\beta = 0.226$$

The correlation coefficient, r^2, for the linear regression was 0,966.

The *combined* centrifuge and C-P cell regression line intersects that of the settling data at a solids compressive pressure of 365,3 Pa. If the centrifuge data are ignored, the regression line of the *combined* C-P cell data intersects that of the settling data at 1 285,1 Pa. Sets of equations (42) and (43) were used for the porosity versus solids compressive pressure relationship in the planar and internal cylindrical filtration models. Set of equations (42) incorporates the centrifuge

data as discussed above, while for set of equations (43) the centrifuge data are ignored. In the same manner as for permeability, the porosity of the cake was assumed to be constant and equal to ϵ_f below P_{s_f}.

$$
\begin{aligned}
1-\epsilon &= 0.0299 P_{s_f}^{0.0782} && 0 \le P_s \le P_{s_f} \\
1-\epsilon &= 0.0299 P_s^{0.0782} && P_{s_f} \le P_s \le 365.3\,\text{Pa} \\
1-\epsilon &= 0.0125 P_s^{0.226} && P_s \ge 365.3\,\text{Pa}
\end{aligned} \tag{42}
$$

$$
\begin{aligned}
1-\epsilon &= 0.0299 P_{s_f}^{0.0782} && 0 \le P_s \le P_{s_f} \\
1-\epsilon &= 0.0299 P_s^{0.0782} && P_{s_f} \le P_s \le 1285.1\,\text{Pa} \\
1-\epsilon &= 0.00785 P_s^{0.265} && P_s \ge 1285.1\,\text{Pa}
\end{aligned} \tag{43}
$$

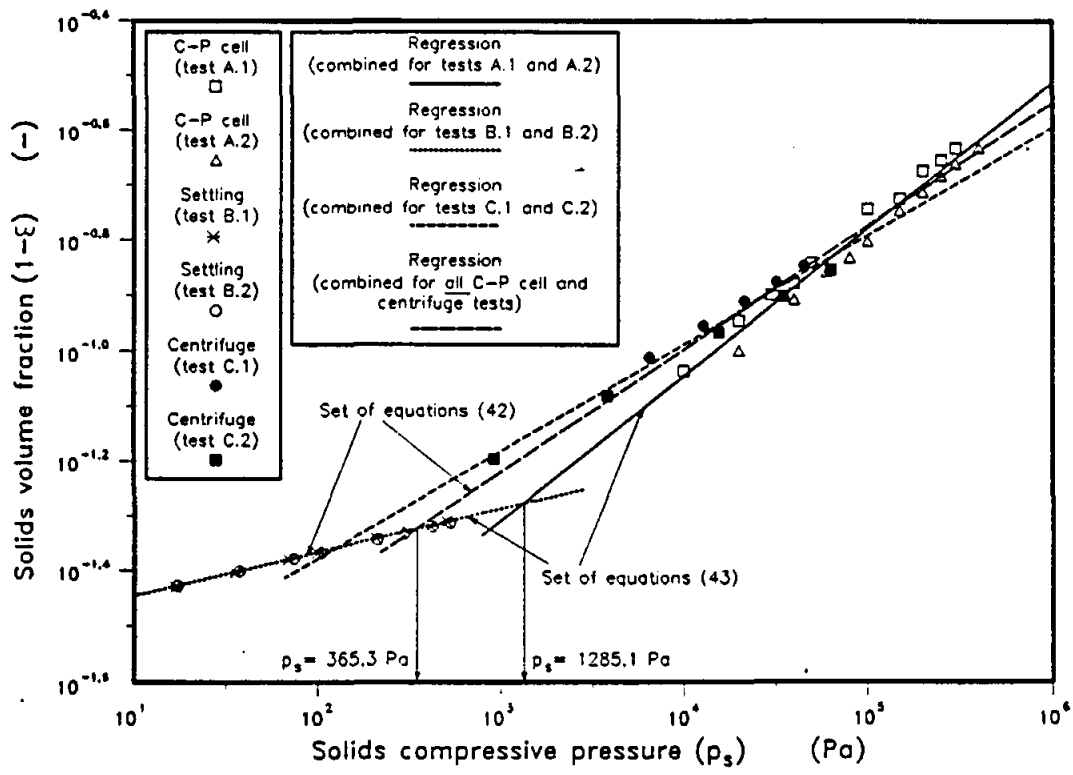

FIGURE 23 **Graph of Solids Volume Fraction ($1-\epsilon$) versus Solids Compressive Pressure (P_s) for the Settling, Centrifuge and C-P Cell Experiments Showing the Basis for Sets of Equations (42) and (43)**

Sets of equations (42) and (43) are similar to set of equations (9), which was proposed by Tiller and Cooper (1962).

As noted in Chapter 4, set of equations (43) gave a better correlation between experimental and predicted average cake dry solids concentrations, when used in the planar and internal cylindrical filtration models, than set of equations (42).

Rencken (1992) attempted to fit all the permeability and porosity data to equations (11) and (12) respectively. Equations (11) and (12) were proposed by Tiller and Leu (1980). However, the fit between a non-linear regression, using equations (11) and (12) and the experimental data, was not very good. Also, when the non-linear regression equations for equations (11) and (12) were incorporated into the planar and internal cylindrical filtration models, the correlation between experimental and predicted values was not very good.

3.3.4.3 Porosity and Permeability Data for Error Analysis

As shown in Figures 14 and 15 for permeability and solids volume fraction $(1-\epsilon)$, respectively, there was a significant "scatter" of experimental points around the regression lines for the *combined* C-P cell data for tests A.1 and A.2.

In an error analyses (Rencken, 1992) it was found that this "scatter" was significant when incorporated into the planar and internal cylindrical filtration models. The error or uncertainty limits for the C-P cell data were determined by using the permeability versus solids compressive pressure relationship for test A.1 with the porosity versus solids compressive pressure relationship for test A.2 and vice versa.

The resultant sets of equations (similar to sets of equations (41) and (43)) for the uncertainty limits are :

$$
\begin{aligned}
1-\epsilon &= 0{,}0299\,P_{s/}^{0.0782} && 0 \le P_s \le P_{s/} \\
1-\epsilon &= 0{,}0299\,P_s^{0.0782} && P_{s/} \le P_s \le 2249.3\,Pa \\
1-\epsilon &= 0{,}00621\,P_s^{0.282} && P_s \ge 2249.3\,Pa \qquad (44)
\end{aligned}
$$

$$\begin{pmatrix} Uncertainty \\ limit\ 1 \end{pmatrix}$$

$$
\begin{aligned}
K &= 6{,}621\times10^{-13}\,P_{s/}^{-0.575} && 0 \le P_s \le P_{s/} \\
K &= 6{,}621\times10^{-13}\,P_{s/}^{-0.575} && P_{s/} \le P_s \le 3567.4\,Pa \\
K &= 2{,}129\times10^{-10}\,P_s^{-1.281} && P_s \ge 3567.4\,Pa
\end{aligned}
$$

$$1-\epsilon = 0{,}0299\,P_{s/}^{0.0782} \qquad 0 \le P_s \le P_{s/}$$

$$1-\epsilon = 0{,}0299\,P_s^{0.0782} \qquad P_{s/} \le P_s \le 1145{,}9\,Pa$$

$$1-\epsilon = 0{,}00771\,P_s^{0.271} \qquad P_s \ge 1145{,}9\,Pa \qquad (45)$$

$$\begin{pmatrix} Uncertainty \\ limit\ 2 \end{pmatrix}$$

$$K = 6{,}621\times10^{-13}\,P_{s/}^{-0.575} \qquad 0 \le P_s \le P_{s/}$$

$$K = 6{,}621\times10^{-13}\,P_{s/}^{-0.575} \qquad P_{s/} \le P_s \le 5245{,}3\,Pa$$

$$K = 2{,}922\times10^{-10}\,P_s^{-1.286} \qquad P_s \ge 5245{,}3\,Pa$$

The basis for sets of equations (44) and (45) is plotted in Figures 24 and 25.

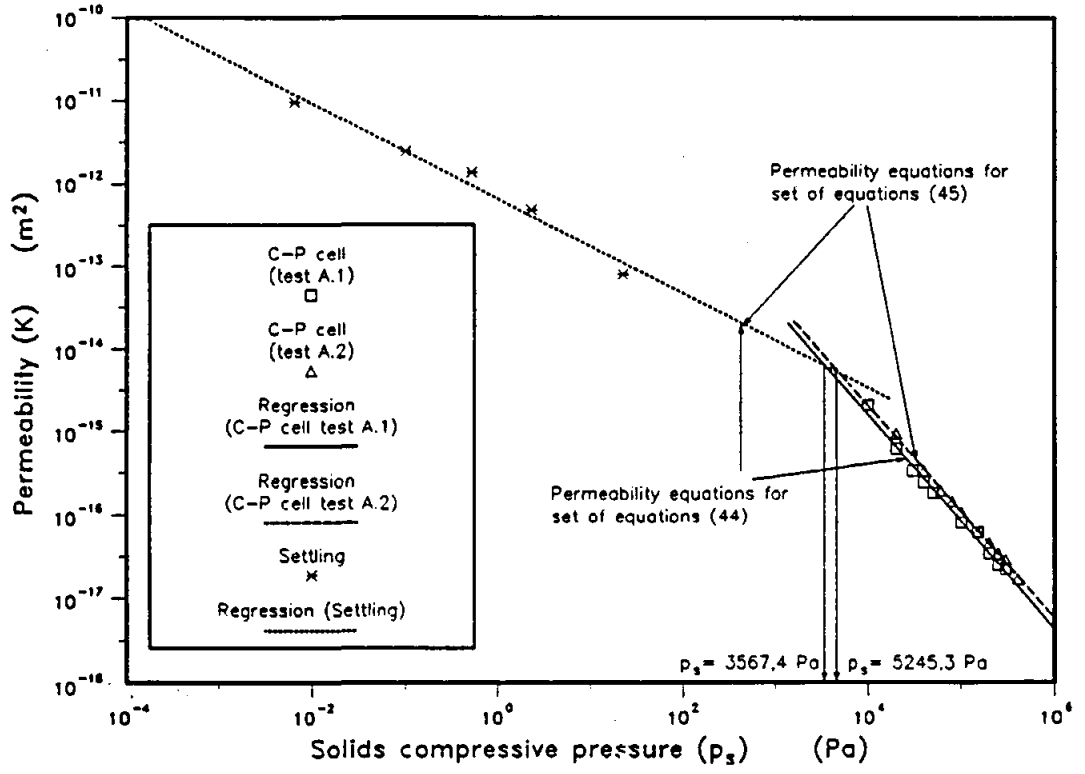

FIGURE 24 **Graph of Permeability (K) versus Solids Compressive Pressure (P_s) for the C-P Cell and Settling Experiments Showing the Basis for Sets of Equations (44) and (45)**

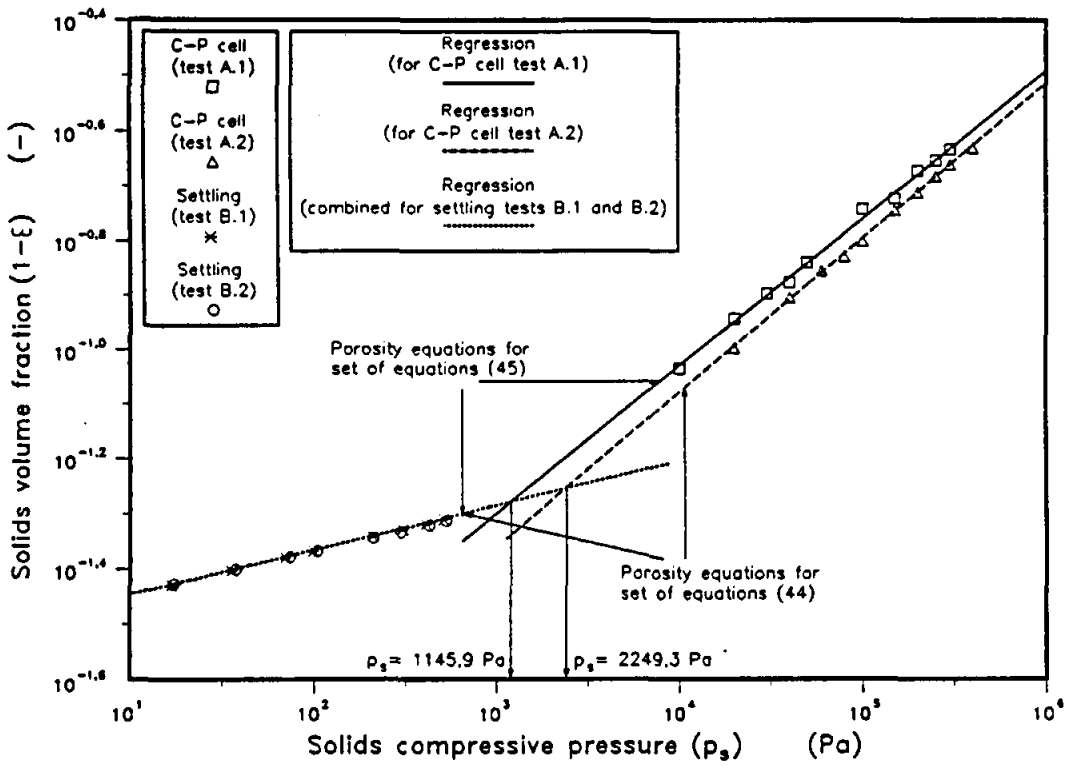

FIGURE 25 **Graph of Solids Volume Fraction ($1 - \epsilon$) versus Solids Compressive Pressure (P_s) for the Settling and C-P Cell Experiments Showing the Basis for Sets of Equations (44) and (45)**

3.4 SUMMARY OF CHAPTER 3

The theory, apparatus and experimental procedure for three characterisation tests, viz. the C-P cell test, the settling test and the centrifuge test, were presented, together with two proposed models to correlate CPV data. The characterisation tests were then applied to a waterworks clarifier sludge.

The results from the individual methods all yielded meaningful trends. The data, in general, fitted the forms of equations (8) to (10). However, as noted in Section 3.3.5, attempts to correlate the data in terms of equations (11) to (13) were unsuccessful.

In general, the results of the centrifuge experiments were inconsistent with those obtained in the C-P cell and the settling tests. A possible reason for this is that the centrifuge test is a relatively new, untested, method and some of the inherent assumptions in the theory could be invalid.

Repeatibility on the C-P cell experiments was not as good as that of the settling tests. This would necessitate multiple sets of C-P cell tests being performed in order to increase confidence in the data.

Chapter 4

PREDICTION OF FILTER PERFORMANCE

The most significant performance factors for filters are the rate of production of filtrate and the average solids content of the cake. Hence, in order to design and optimise filtration systems, it is necessary to be able to predict these performance indicators. Furthermore, in instances where the fracture of cake layers due to tangential shears is likely to be important, e.g. in the TFP, it is also necessary to determine the voidage and solids compressive pressure through the cake.

In this chapter, the utilisation of C-P data to predict filter performance is illustrated. In Section 4.1, the appropriate equations and a proposed solution procedure are presented. For the derivation of the equations the reader is referred to Rencken (1992). In Sections 4.2 and 4.3, the C-P data obtained in Chapter 3 are used to predict the flux-time relationships and average cake solids contents for planar and internal cylindrical filtration respectively. These predicted values are compared to results obtained from experiments on the waterworks clarifier sludge. In Section 4.4, the use of the equations as an analytical tool is illustrated. The CPV data from Chapter 3 is used to predict the performances of planar, internal cylindrical and external cylindrical filtration, and these are contrasted to indicate the optimal filtration geometry for the sludge.

4.1 EQUATIONS

4.1.1 Relationships between P_s and P_l

For a planar cake the relationship was derived in Section 2.2, i.e.

$$\frac{dP_s}{dx} + \frac{dP_l}{dx} = 0 \qquad (5)$$

The initial conditions for equation (5) are :

$$P_s(at\ cake\ surface) = 0$$

$$P_l(at\ cake\ surface) = P \qquad (46)$$

For a cake formed on a cylindrical surface, some of the applied stress is transmitted in the azimuthal direction (*hoop stresses*) (Tiller and Yeh, 1985). The appropriate force balance is depicted in Figure 26.

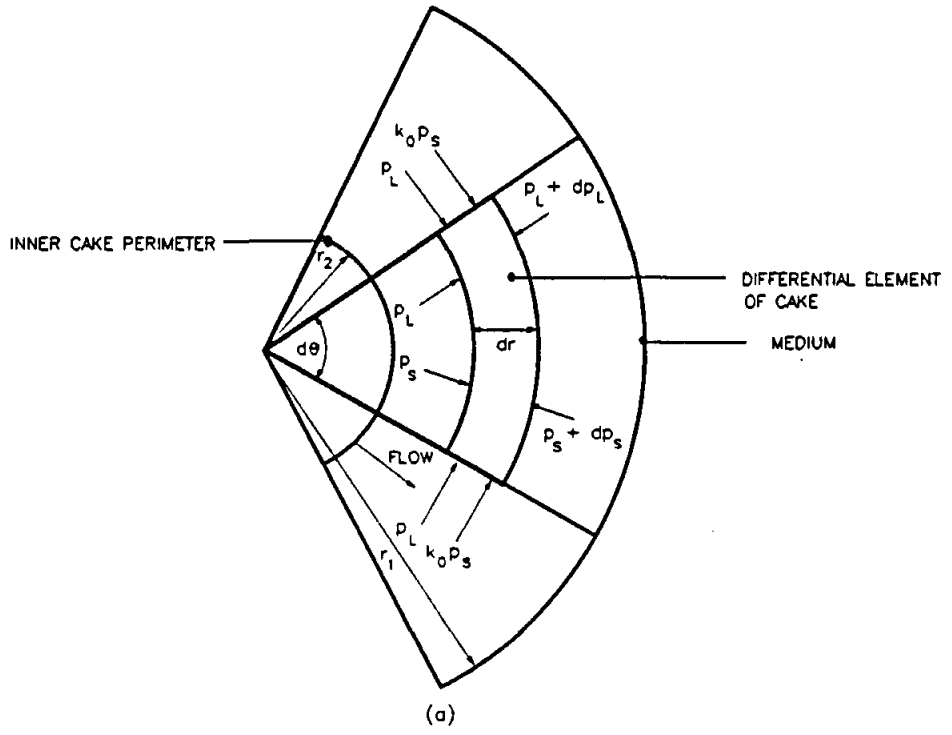

FIGURE 26 **Schematic Diagram of Forces Acting on a Differential Element of Cake for Internal Cylindrical Filtration**

The P_s/P_L relationship is given by (Rencken, 1992):

$$\frac{dP_s}{dr} + \frac{dP_L}{dr} + (1-k_0)\frac{P_s}{r} = 0 \qquad (47)$$

where k_0 = coefficient of earth pressure at rest

For *external* cylindrical filtration, the initial values for equation (47) are :

$$P_s(r_1) = 0$$
$$P_L(r_1) = P \qquad (48)$$

and for *internal* cylindrical filtration, the initial values are :

$$P_s(r_2) = 0$$
$$P_L(r_2) = P \qquad (49)$$

where r_1 and r_2 are defined as in Figure 26.

4.1.2 Pressure Drop Relationships

For a planar cake, the pressure drop across a differential element of cake is given by :

$$\frac{dP_L}{dx} = \frac{\mu \ Q_f}{A \ K}$$

For *external* cylindrical filtration the appropriate equation is :

$$\frac{dP_L}{dr} = \frac{\mu \ Q}{2\pi \ r \ K} \tag{50}$$

and for *internal* cylindrical filtration the appropriate equation is :

$$\frac{dP_L}{dr} = - \frac{\mu \ Q}{2\pi \ r \ K} \tag{51}$$

In equations 50 and 51, the direction of increasing r is defined in Figure 26.

The overall pressure balance for both planar and cylindrical coordinate systems is given by :

$$P = \Delta P_c + \Delta P_m \tag{52}$$

where ΔP_c = pressure drop across the cake (Pa)

ΔP_m = pressure drop across the medium (Pa)

For planar filtration the pressure drop across the medium is defined (Leu, 1981) as :

$$\Delta P_m = \frac{\mu_f Q_f R_m}{A} \tag{53}$$

where ΔP_m = pressure drop across the medium, (Pa)

R_m = resistance of medium, (m^{-1})

In the same manner the pressure drop across the medium for cylindrical filtration is :

$$\Delta P_m = \frac{\mu_f Q_f R_m}{2\pi r_1 l} \tag{54}$$

4.1.3 Mass Balances

Once the solids compressive pressure profile through the cake has been calculated, the porosity profile may be obtained by using an empirical equation such as equation (3.33) or (3.36).

The average porosity is given by :

$$\epsilon_{av} = \frac{2\pi \int_{r_2}^{r_1} \epsilon r dr}{\pi (r_1^2 - r_2^2)} \tag{55}$$

where ϵ_{av} = average porosity of cake, (-)

Since the solids and liquid are incompressible, a total mass balance on a volumetric basis gives :

$$\left\{\begin{matrix}\textit{Volume of}\\ \textit{slurry per unit}\\ \textit{medium area}\end{matrix}\right\} = \left\{\begin{matrix}\textit{Volume of}\\ \textit{cake per unit}\\ \textit{medium area}\end{matrix}\right\} + \left\{\begin{matrix}\textit{Volume of}\\ \textit{filtrate per unit}\\ \textit{medium area}\end{matrix}\right\}$$

or

$$\frac{\omega_c}{\phi_s} = \frac{\omega_c}{(1-\epsilon_{av})} + v \tag{56}$$

where ϕ_s = volume fraction of solids in feed sludge (-)

ω_c = volume of cake dry solids per unit medium area (m^3/m^2)

Also,

$$\omega_c = \frac{(1-\epsilon_{av})(r_1^2 - r_2^2)}{2r_1} \tag{57}$$

Solving for v using equations (56) and (57) gives :

$$v = \frac{(1-\epsilon_{av}-\phi_s)}{\phi_s}\frac{(r_1^2 - r_2^2)}{2r_1} \tag{58}$$

4.1.4 Time Relationships for Constant Pressure Filtration

For constant pressure filtration, filtration time is calculated from equation (59) :

$$t = \int_0^V \frac{dV}{Q} \tag{59}$$

where V = volume of filtrate per unit length of tube, (m^3/m)

Numerical integration of equation (59) requires that Q be known as a function of V. V may be calculated from equation (58) :

$$V = \frac{(1 - \epsilon_{av} - \phi_s)\pi(r_1^2 - r_2^2)}{\phi_s} \qquad (60)$$

4.1.5 Solution Procedure

A proposed solution algorithm for the filtration equations is as follows :

(i) Specify cake thickness

(ii) Solve for Q_f

- (a) Assume Q_f
- (b) Calculate ΔP_m
- (b) Integrate P_s/P_L profile equations (equations (5) and (1), equations (47) and (50) or equations (47) and (51)) using the permeability relationships (equation (8)). Hence calculate ΔP_c
- (c) Iterate Q_f until equation (52) is solved

(iii) From P_s profile and voidage relationship (equation (9)) calculate voidage profile through cake. Hence calculate average porosity from equation (55)

(iv) Calculate V from equation (60)

(v) Calculate t from equation (59)

This yields values for ϵ_{av}, Q_f and t for the specified cake thickness. By repeating the procedure for various cake thicknesses, the profiles that ϵ_{av} and Q_f exhibit with time is obtained.

4.2 RESULTS : CONSTANT PRESSURE PLANAR FILTRATION

Constant pressure planar filtration experiments were conducted on the waterworks clarifier sludge. The apparatus and results are presented in Rencken (1992). The experiments were conducted at three filtration pressures, namely, 100 kPa, 200 kPa and 300 kPa, and the solids concentration of the feed sludge was approximately 49 g/ℓ.

On solving the model for planar filtration, it was found that the discrepancy between predicted and experimental cake solids was significant when the results of the centrifuge experiments were included. This is consistent with the findings in Chapter 3, i.e. that the results from the centrifuge experiments were somewhat inconsistent with that obtained in the C-P cell and the settling tests. The data obtained from the centrifuge experiments were subsequently excluded. Hence, the CPV data used in predictions was obtained from the C-P cell and the settling tests only.

The predicted average cake solids are compared to experimentally measured values in Figure 27. Almost all the experimental average cake dry solids concentrations fall within the range of uncertainty for the model predictions. The uncertainty limits shown in Figures 27(b) to (d) were determined by using sets of equations (44) and (45) to describe the variation of permeability and porosity with solids compressive pressure in the planar model (see Section 3.3.4.3).

The predicted and experimental filtrate fluxes are shown in Figures 28(a) to (d). As shown in Figure 28(a) there was only a marginal increase in filtrate flux with filtration pressure, confirming that for the highly compressible waterworks sludge, the flux is relatively independent of operating pressure (see Section 2.3.2). Except for a few experimental points for P = 100 kPa, all the experimental filtrate fluxes fell within the range of uncertainty for the model predictions.

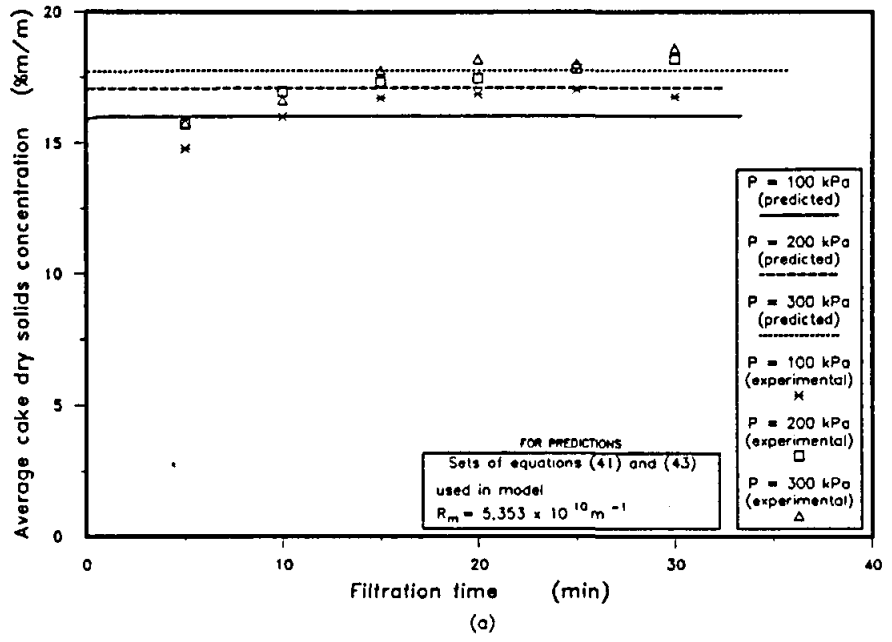

(a)

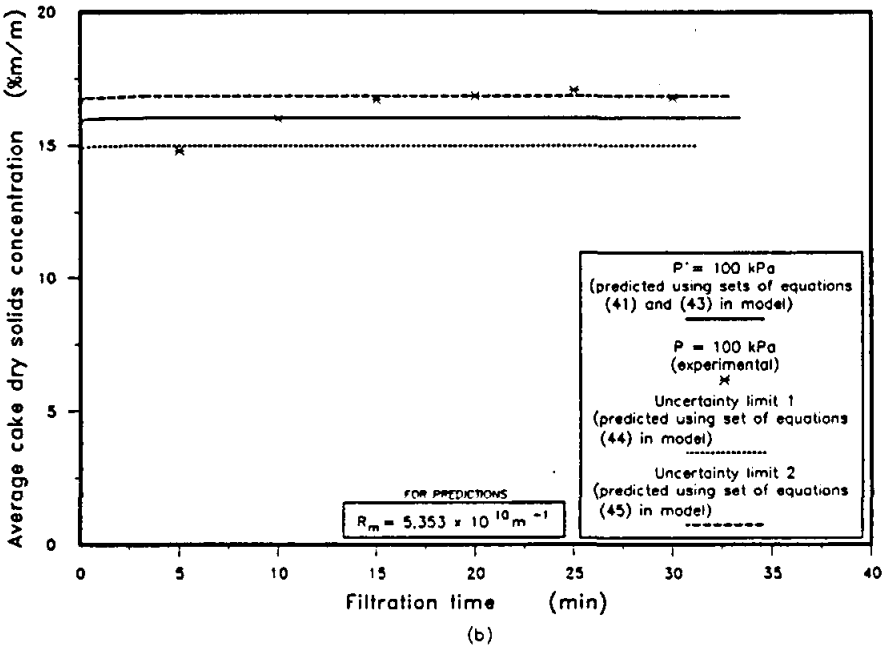

(b)

FIGURE 27 (a) and (b)

Comparison Between Experimental and Predicted Average Cake Dry Solids Concentrations for Planar Filtration (Centrifuge Data Excluded) :

(a) Combined Results;

(b) Individual Results for P = 100 kPa

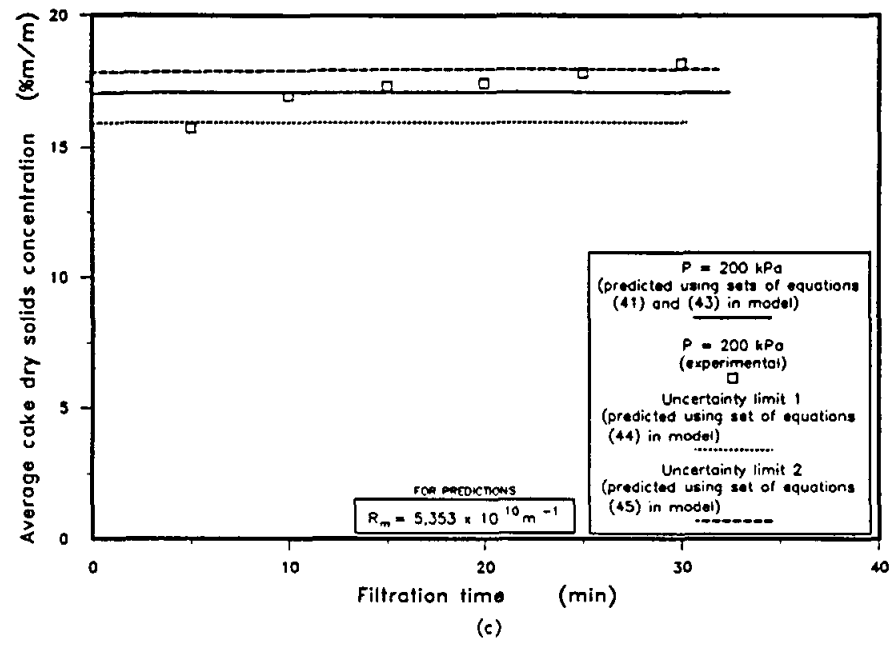

(c)

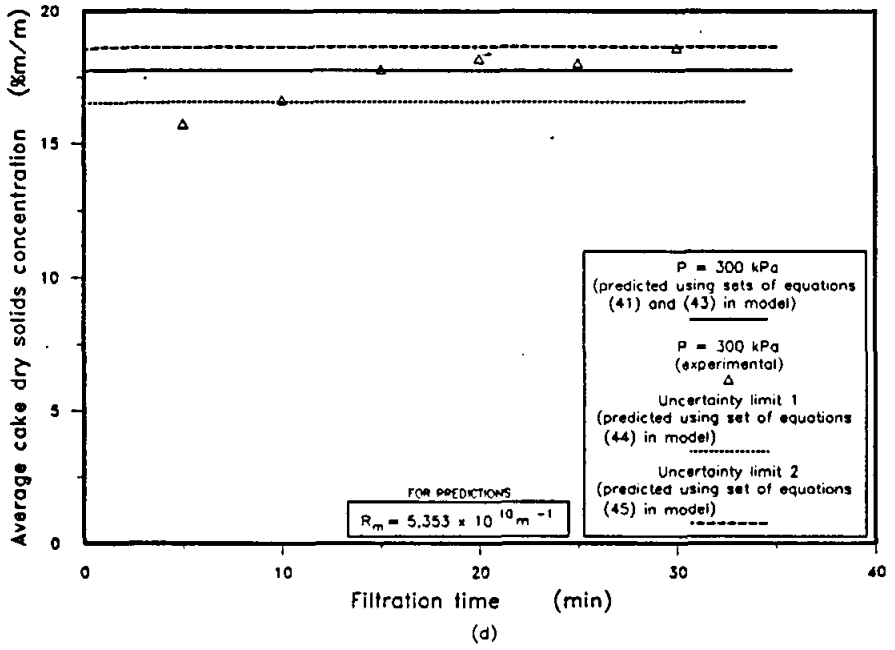

(d)

FIGURE 27 (c) and (d)

Comparison Between Experimental and Predicted Average Cake Dry Solids Concentrations for Planar Filtration (Centrifuge Data Excluded) :

(c) and (d) Individual Results for P = 200 kPa and P = 300 kPa respectively.

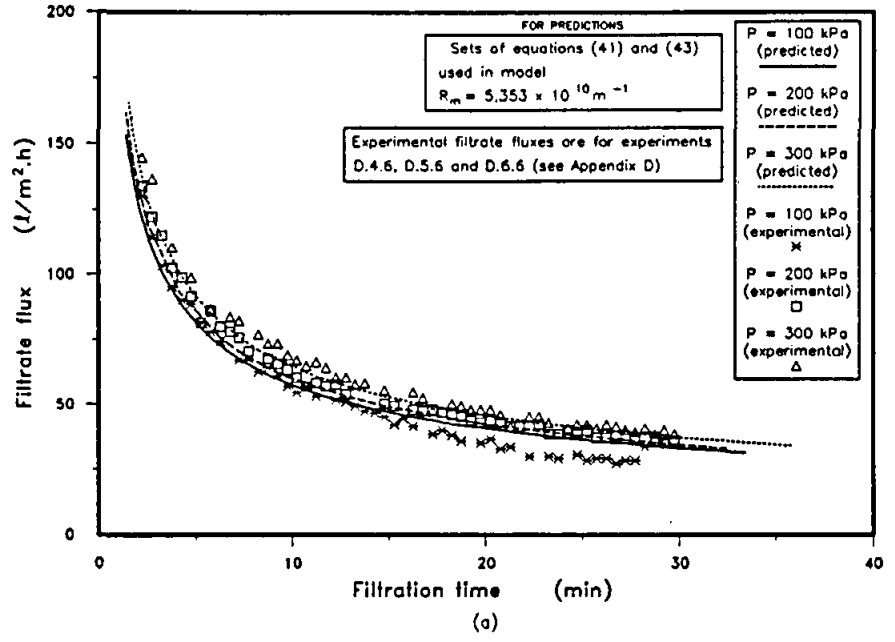

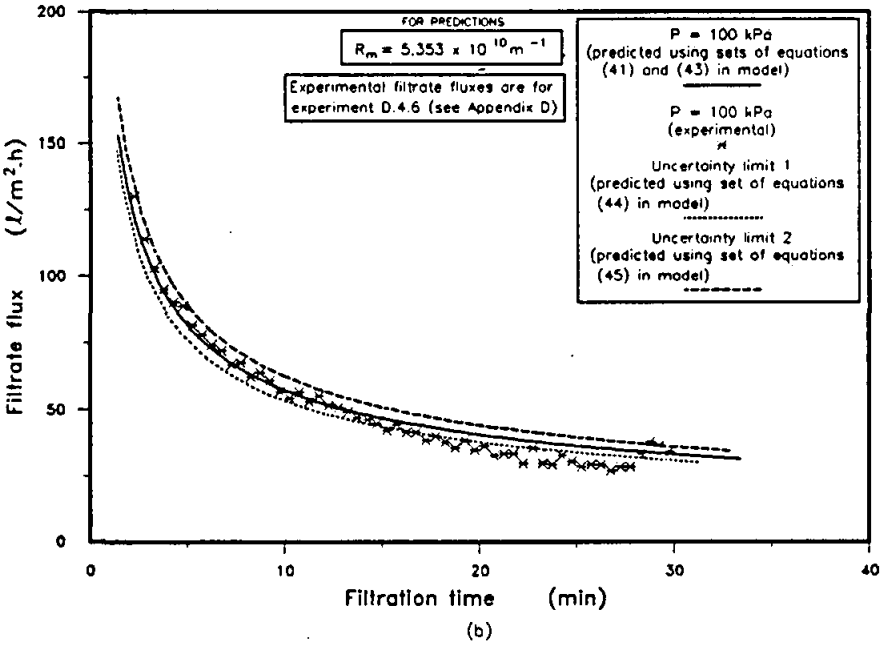

FIGURE 28 (a) and (b)

Comparison Between Experimental and Predicted Filtrate Fluxes for Planar Filtration :

(a) Combined Results;

(b) Individual Results for P = 100 kPa

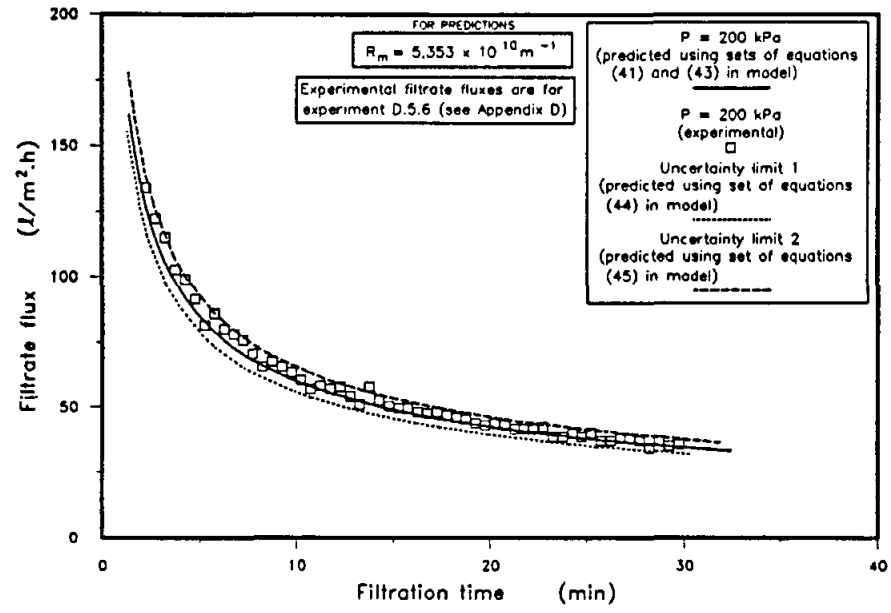

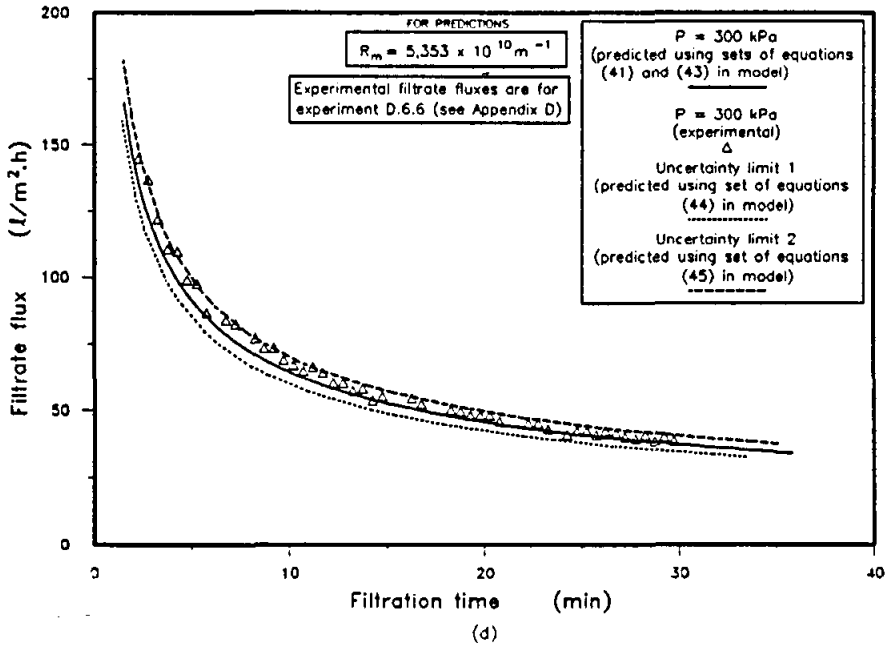

FIGURE 28 (c) and (d)

Comparison Between Experimental and Predicted Filtrate Fluxes for Planar Filtration :
(c) and (d) Individual Results for P = 200 kPa and P = 300 kPa, respectively

4.3 RESULTS : INTERNAL CYLINDRICAL FILTRATION

Three series of experiments using the waterworks sludge were performed on the TFP at filtration pressures of 100 kPa, 200 kPa and 300 kPa. The details of the apparatus are presented in Rencken (1992).

The value of k_o (see equation 47) was taken to be 0,34. This was the same value Tiller and Lu (1972) had measured for Solkafloc, which is also a very compressible material. It was established that the value of k_o has no great effect on the results generated by the internal cylindrical filtration model, except for small cake diameters or long filtration times (Rencken, 1992). Tiller and Yeh (1985) found that for external cylindrical filtration the effect of k_o was also not very significant.

The experimental average cake dry solids concentrations at various filtration times for filtration pressures of 100 kPa, 200 kPa and 300 kPa are shown in Figure 29(a), together with the predictions of the internal cylindrical filtration model. The results of three experiments to determine repeatability, showed that the maximum deviation of the average cake dry solids concentrations was 3,14 %. The degree of uncertainty in the experimental values is shown in Figures 29(b), (c) and (d) by means of error bars for P = 100 kPa, 200 kPa and 300 kPa, respectively.

As discussed in Section 3.3.4.3, there was a significant "scatter" in the experimental results of the two C-P cell tests. The uncertainty limits for the C-P cell data shown in Figures 29(b) to (d), were determined by using sets of equations (44) and (45) to describe the variation of permeability and porosity with solids compressive pressure, in the model. As shown in Figures 29(b) to (d) the experimental results fell within this uncertainty range.

There was a good fit between the experimental values for filtration flux and those determined by the internal cylindrical filtration model, for all three pressures which were investigated. This is shown in Figures 30(a) to (d). The experimental results fell within the uncertainty range for the C-P cell data, as determined by sets of equations (44) and (45).

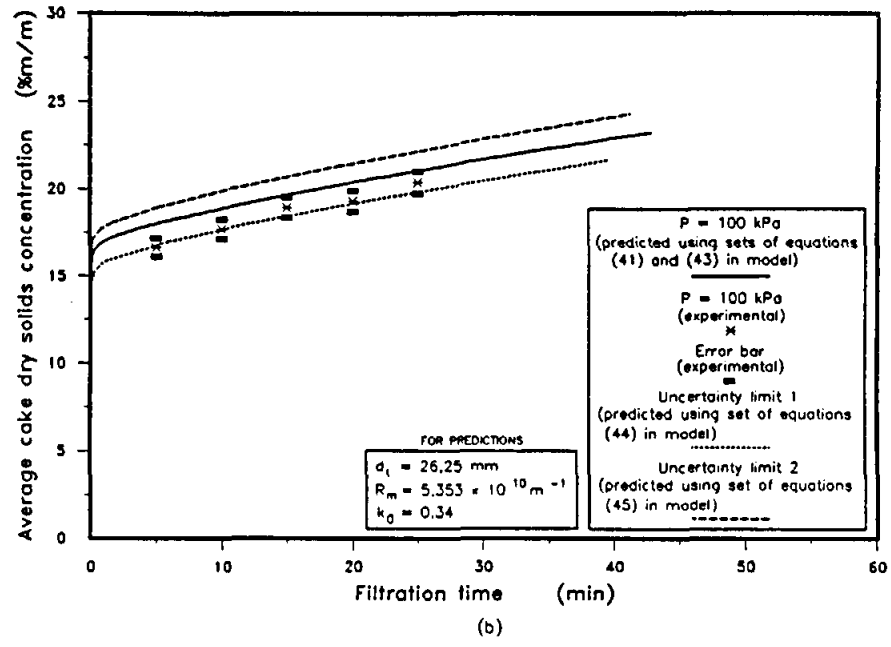

(b)

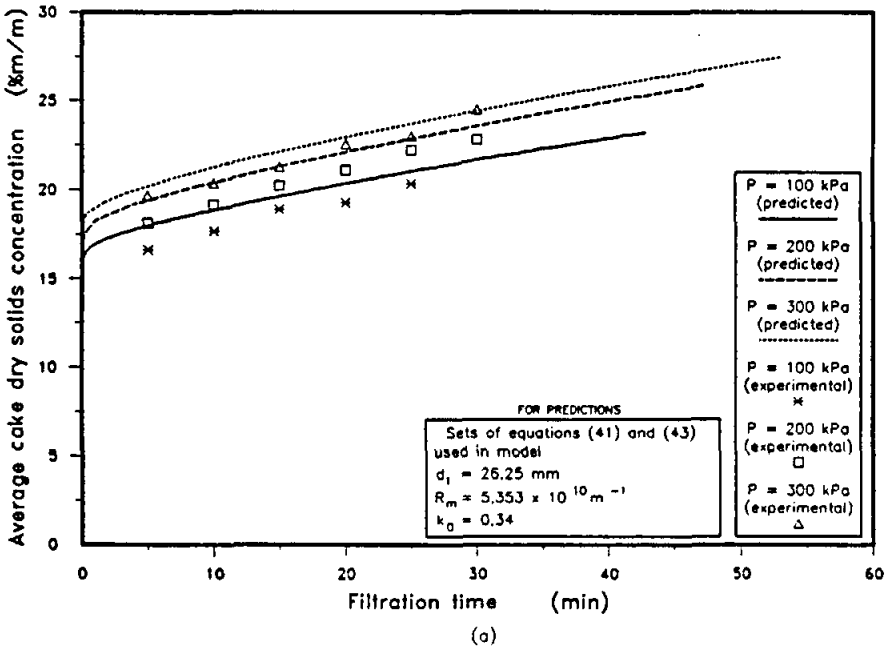

(a)

FIGURE 29 (a) and (b) **Comparison Between Experimental and Predicted Average Cake Dry Solids Concentrations for Internal Cylindrical Filtration (Centrifuge Data Excluded) :**
(a) Combined Results
(b) Individual Results for P = 100 kPa

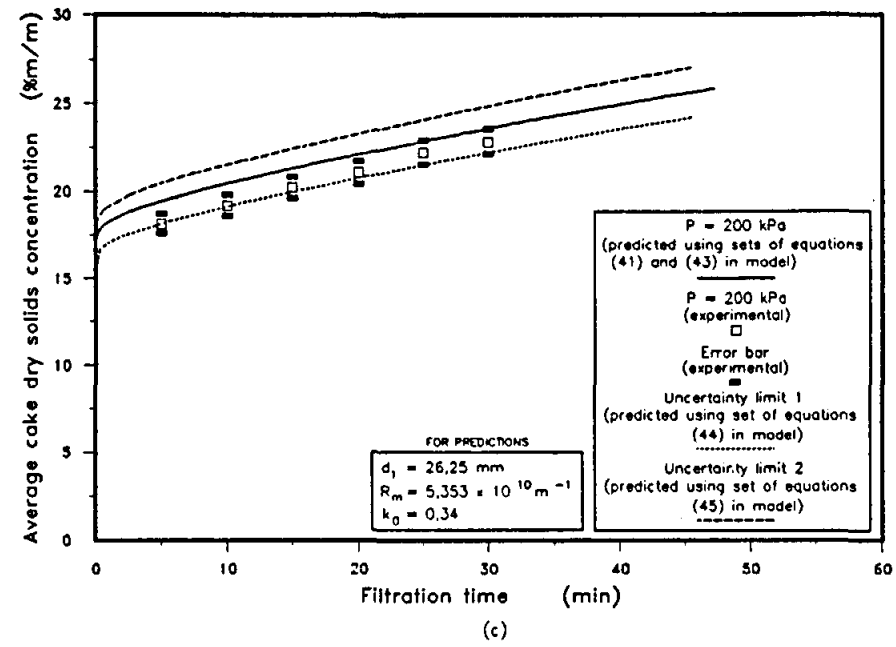

(c)

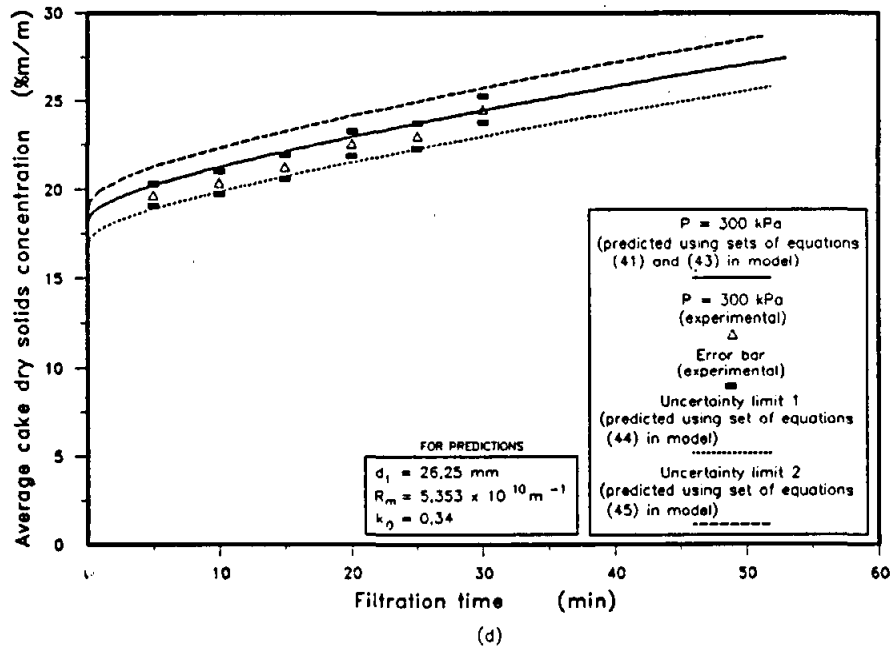

(d)

FIGURE 29 (c) and (d)

Comparison Between Experimental and Predicted Average Cake Dry Solids Concentrations for Internal Cylindrical Filtration (Centrifuge Data Excluded) :
(c) and (d) Individual Results for P = 200 kPa and P = 300 kPa, respectively

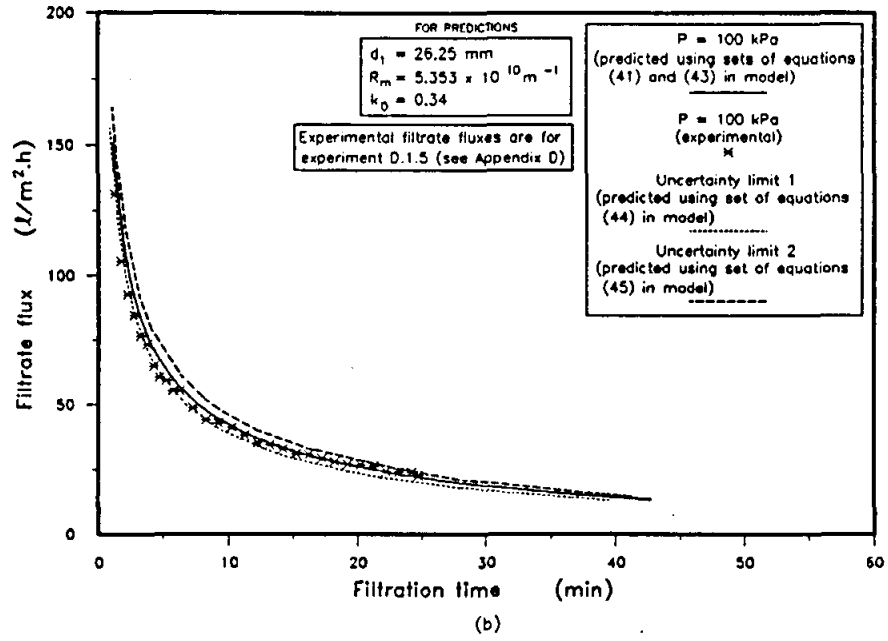

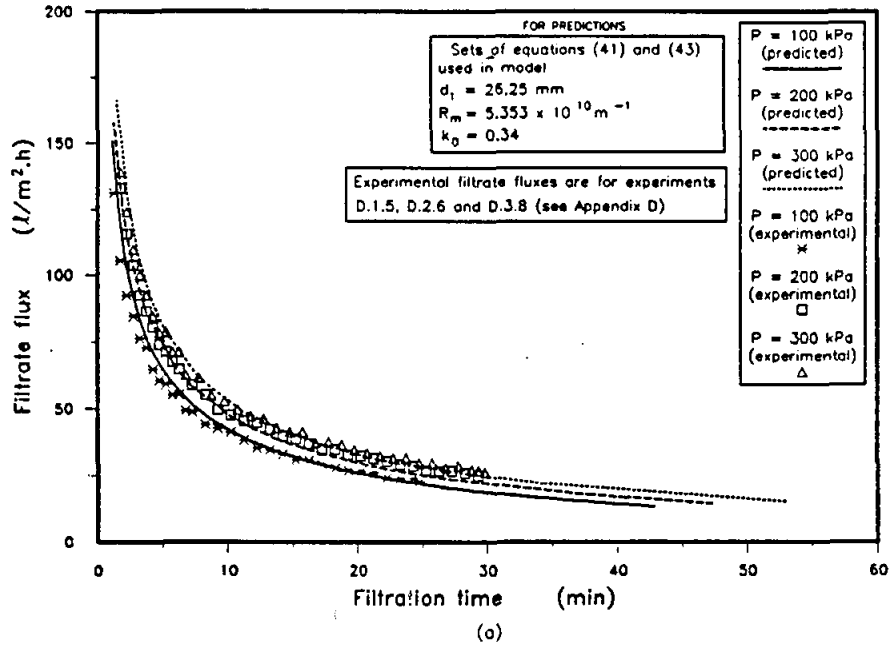

FIGURE 30 (a) and (b)

Comparison Between Experimental and Predicted Filtrate Fluxes for Internal Cylindrical Filtration :

(a) Combined Results

(b) Individual Results for P = 100 kPa

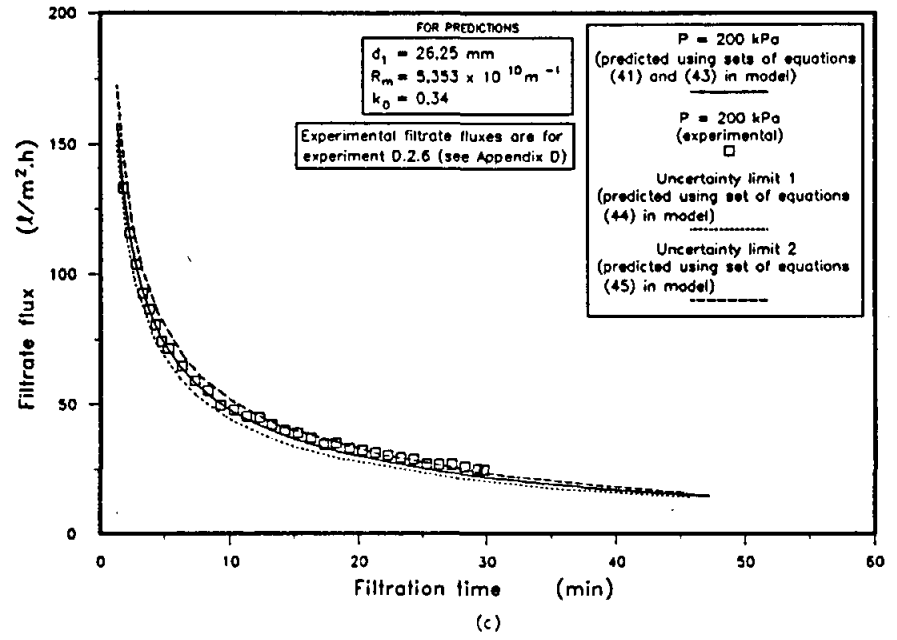

(c)

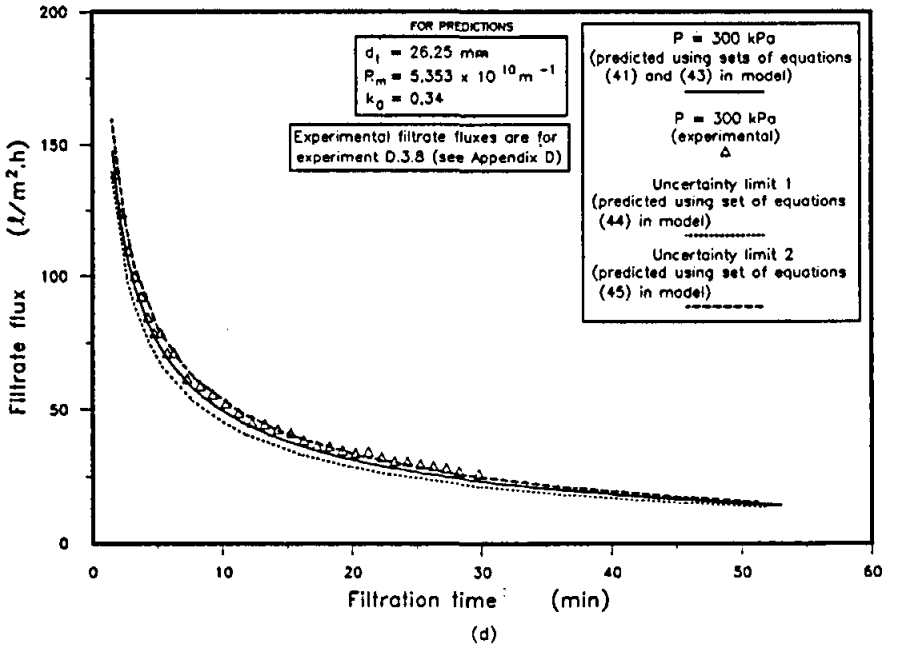

(d)

FIGURE 30 (c) and (d)

Comparison Between Experimental and Predicted Filtrate Fluxes for Internal Cylindrical Filtration :
(c) and (d) Individual Results for P = 200 kPa and P = 300 kPa, respectively

4.4 COMPARISON BETWEEN EXTERNAL CYLINDRICAL, INTERNAL CYLINDRICAL AND PLANAR FILTRATION

A comparison between the average cake dry solids concentrations for external cylindrical, internal cylindrical and planar filtration of the waterworks sludge, is shown in Figure 31. For internal cylindrical filtration and planar filtration the *experimental* and *predicted* values are shown, while for external cylindrical filtration the values were only *predicted*.

The cake thickness for external cylindrical filtration was defined as, $r_4 - r_3$, while that for internal cylindrical filtration was defined as, $r_1 - r_2$. For external cylindrical filtration, r_3 is the external radius of the filter medium.

As shown in Figure 31, for very small cake thicknesses, the average cake dry solids concentration is approximately the same for all three filtration configurations. As the cake thickness increases, the average cake dry solids concentration for internal cylindrical filtration increases, that for planar filtration remains essentially constant, while for external cylindrical filtration the average cake dry solids concentration decreases.

These trends may be explained as follows. A well consolidated cake skin with a high resistance forms near the filter medium. The bulk of the cake, however, consists of "sloppy" cake which is not well consolidated or compressed. For external cylindrical filtration the outer diameter increases (cake thickness increases) as the filtration progresses. As the external diameter increases, the mass of the "sloppy" outer cake layers as a fraction of the total cake mass increases, while the mass fraction of the relatively well consolidated inner cake layers decreases. Thus the *average* cake dry solids concentration decreases as the cake thickness increases. For internal cylindrical filtration the converse is true. The mass fraction of the "sloppy" inner cake layers decreases as the internal cake diameter decreases and the cake thickness increases. The increase in P_s throughout the bulk of the cake, as the internal cake diameter decreases, further contributes to an increase in average cake dry solids concentration for small internal cake diameters. This is probably the cause of the slight upwards turn in the internal cylindrical filtration curve in Figure 31, for large cake thicknesses (small internal cake diameters).

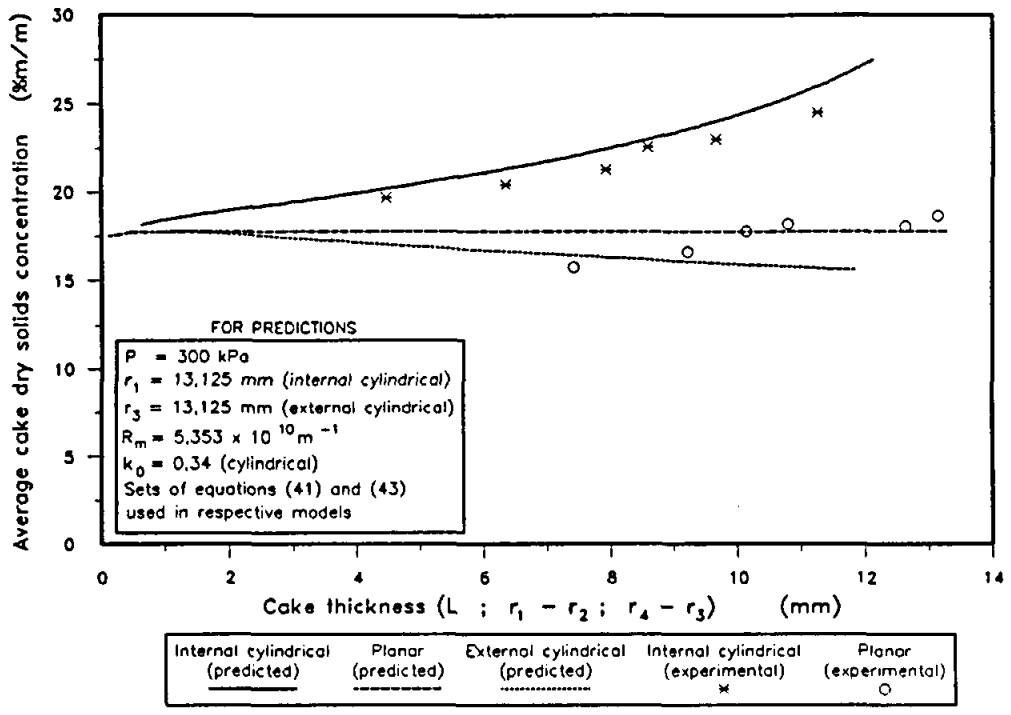

FIGURE 31 **The Variation of Average Cake Dry Solids Concentration with Cake Thickness for External Cylindrical, Internal Cylindrical and Planar Filtration**

For planar filtration, the mass of the "sloppy" cake layers as a fraction of the total mass of cake, remains essentially constant, irrespective of cake thickness. Therefore the average cake dry solids concentration remains essentially constant.

The variation of cake thickness with filtration time for the waterworks clarifier sludge is shown in Figure 32 for all three filtration configurations. For internal cylindrical and planar filtration the *experimental* and *predicted* values are shown, while for external cylindrical filtration the values were *predicted*. For small cake thicknesses, there is no significant difference between the three configurations. For greater cake thicknesses, the filtration time for internal cylindrical filtration is higher than that for external cylindrical and planar filtration. This is due to the significant reduction in filtration area, for large cake thicknesses, during internal filtration.

The variation of dry solids production rate with cake thickness for the waterworks clarifier sludge is shown in Figure 33, for the three filtration configurations. For internal cylindrical and planar filtration the *experimental* and *predicted* dry solids production rates are shown, while for external cylindrical filtration the dry solids production rates were *predicted*. The dry solids production rate in Figure 3.49 was defined as :

$$\textit{Dry solids production rate } (kg/m^2.h) = \frac{\textit{Mass of dry solids in cake for certain cake thickness}}{(\textit{Area of filter medium} \times \textit{Filtration time})} \qquad (61)$$

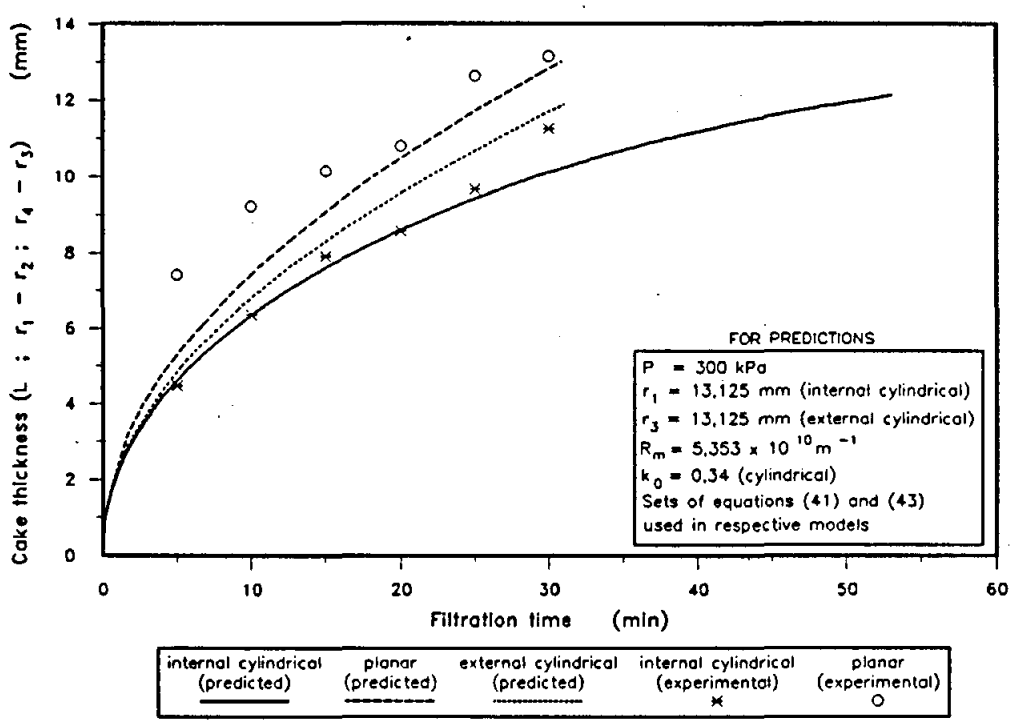

FIGURE 32 **Graph of Cake Thickness versus Filtration Time for External Cylindrical, Internal Cylindrical and Plana Filtration**

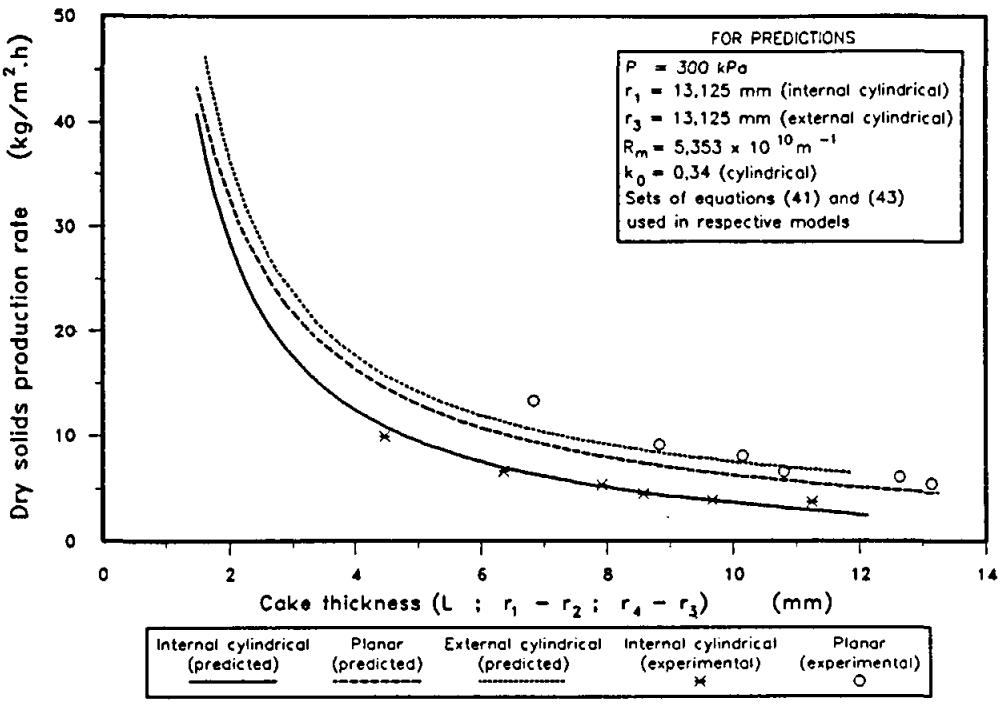

FIGURE 33 **Graph of Dry Solids Production Rate versus Cake Thickness for External Cylindrical, Internal Cylindrical and Planar Filtration**

This definition of dry solids production rate is based on filtration time only and ignores time for cake removal which would be required in practice. Any cake losses due to cake removal are also ignored.

The dry solids production rate for external cylindrical filtration is slightly higher than that for planar filtration. This is due to the increase in external filter area as cake thickness increases.

The dry solids production rate for internal cylindrical filtration is close to that for planar filtration, for small cake thicknesses. For greater cake thicknesses the dry solids production rate for internal cylindrical filtration is significantly lower than that for planar filtration. This is due to the decrease in internal filtration area as cake thickness increases.

4.5 SUMMARY OF CHAPTER 4

The relevant filtrations equations were presented, together with a solution algorithm. CPV data for the waterworks clarifier sludge was utilised to predict the performance of a planar and an internal cylindrical filter. This was then compared to results obtained experimentally.

When the combined C-P cell, settling test and centrifuge data was utilised, the comparison between predicted and experimental was not as good as when the centrifuge data was excluded. Then, the predicted filtrate fluxes and cake solids contents were very close to the experimental values.

The results obtained in this chapter indicate that the performance of filters may reasonably be predicted from solving the appropriate filtration equations with experimentally obtained characterisation data.

Chapter 5

CONCLUSION

The aim of this study is to acquaint workers in the water field with the effects associated with compressible cakes, and to identify and develop methodology that would enable workers to characterise compressible cakes and predict the performance of large scale filters from laboratory tests.

The major cause of cake compression in filters is hydraulic compression, where fluid frictional forces cause particles to irreversibly infiltrate existing void spaces, leading to a more densly packed cake of reduced voidage and permeability. Hydraulic compression causes solids compressive pressure profiles to be established within the cake, the compressive pressure being zero at the cake surface and progressively increasing towards the filtration medium. The solids compressive pressure, in turn, establishes voidage, permeability and critical shear stress profiles through the cake. The voidage and permeability are high at the cake surface and decrease towards the filtration medium. The critical stress is an indication of the cakes resistance to fracture by tangential shear forces. The critical shear stress is low at the cake surface and increases towards the filtration medium. The shapes of the profiles is determined by the extent of compressibility of the cake.

This hydraulic compression of the cake has various effects on the cake properties and the filter performance. These include the *skin effect*, where most of the resistance of the cake becomes confined to a thin skin adjacent to the filtration medium. The skin has a low voidage and is highly consolidated, whereas the rest of the cake is "sloppy" with a high moisture content and a low resistance to tangential shears. The hydraulic compression effect also results in highly compressive cakes becoming insensitive to operating conditions, e.g. increases in operating pressure do not result in an increase in filtrate production or in the cake solids content. A further effect of hydraulic compression is that the filter performance may become dependent on the operating path taken to reach the operating point. The cake "remembers" the worst conditions that it was exposed to, and maintains a resistance appropriate to that worst condition, irrespective of subsequent improvements in operating conditions. This emphasises the necessity for better control of filtration systems.

Characterisation of compressible cakes resolves to quantifying the permeability - compressive pressure and the voidage - compressive pressure relationships (herein collectively termed *CPV data*). Various models to correlate CPV data were identified. However, model parameters must be evaluated by laboratory tests. Three methods to quantify CPV data were investigated, viz. the compression-permeability (C-P) cell, settling tests and the centrifuge test. The C-P cell was proposed to obtain CPV at high compressive pressures, the settling tests at low

compressive pressures and the centrifuge test at intermediate pressures. The theory, apparatus and experimental procedures for each test were presented. The tests were then applied to obtain CPV data for a waterworks clarifier sludge obtained from Umgeni Water's H D Hill Water Treatment Plant.

Two sets of experiments were performed for each method, in order to determine the repeatibility. The results for the settling tests and the centrifuge tests were highly repeatable. The results for the C-P cell were less so, necessitating the specification of a confidence interval in subsequent utilisation of the data. The results obtained on all three methods individually fitted the correlative models well. When the results from the three methods were combined, however, the results obtained on the centrifuge tests differed from that obtained via the C-P cell test and the settling test. This called into question the centrifuge test as a method to characterise the sludge.

Prediction of filter performance, i.e. the filtrate flux and cake solids content, requires the CPV data for the sludge as well as filtration equations appropriate to the geometry of the filter. The filtration equations for three common geometries were presented, viz. planar filtration, filtration on an internal cylindrical surface and filtration on an external cylindrical surface. The equations for filtration of compressible cakes on an internal cylindrical surface had not previously been reported in the literature, and were developed during the course of this study. An algorithm for the solution of the equations was proposed.

The use of the equations was illustrated. The change in filtration flux and average cake solids with time was predicted for planar and internal cylindrical filtration, using the CPV data obtained on the waterworks sludge. This was then compared to experimental data obtained on a planar filter and the tubular filter press (internal cylindrical filtration). The comparison between predicted and experimental values is extremely good.

The use of the equations as an analytical tool was also illustrated. The CPV data was utilised to predict performances for planar, internal cylindrical and external cylindrical filtration. The comparison indicated that, *inter alia*, for a given cake thickness the average cake solids obtained in internal cylindrical filtration could be significantly greater than that obtained in planar or external cylindrical filtration.

Overall, the study indicated that good prediction of filtration performance is feasible if reliable CPV data is employed in the appropriate filtration equations.

Chapter 6

RECOMMENDATIONS

1 Determination of Compression-Permeability-Voidage Relationships From Operating Plant Data

This study has illustrated that effective prediction of plant performance may be obtained by utilising experimental CPV data in the appropriate filtration equations. It is likely that in many water works workers may lack the equipment, time and skill to perform characterisation tests on their sludge. Hence, the feasibility of obtaining CPV data from filtrate fluxes and cake solids contents obtained from operating plants should be investigated. This is likely to necessitate elaborate and complex numerical procedures and computational skills. However, if feasible, the reward would be that basic CPV data may be obtained from existing plant records, whereafter improvements to the process may be computationally investigated.

2 Development of a Guide and Computer Software

In instances where workers are able to perform the characterisation tests, they could still face a problem in solving the appropriate filtration equations, since this requires a knowledge of programming and numerical solution techniques. Hence, it would be of benefit to the water industry if the solution procedures were coded into *user friendly* computer software that would run on a personal computer. This, in combination with a step-by-step Guide to sludge characterisation, could extend the applications of this work.

SELECTED BIBLIOGRAPHY

LEU, W. F. (1981). **Cake Filtration,** Ph.D. Thesis, Department of Chemical Engineering, University of Houston

MICHAELS, A. S. and BOLGER, J. C. (1962). **Settling Rates and Sediment Volumes of Flocculated Kaolin Suspensions,** *Industrial and Engineering Chemistry Fundamentals*, 1(1), pp. 24-33

MURASE, T., HAYASHI, N., SUZUKI, H. and SHIRATO, M. (1985). **Two-dimensional Expression on a Cylindrical Filter Element,** *International Chemical Engineering*, 25(1), pp. 130-137

MURASE, T., IWATA, M., ADACHI, T., GMACHOWSKI, L. and SHIRATO, M. (1989). **Ab Evaluation of Compression-Permeability Characteristics in the Intermediate Concentration Range by Use of Centrifugal and Constant-rate Compression Techniques,** *Journal of Chemical Engineering of Japan*, 22(4), pp. 378-384

PERRY, R. H. and CHILTON, C. H. (1973). *Chemical Engineer's Handbook*, 5th Edition, McGraw Hill Kogakusha Ltd., Tokyo

PILLAY, V. L. (1992). **Modelling of Turbulent Cross-flow Microfiltration of Particulate Suspensions,** Ph.D. Thesis, Department of Chemical Engineering, University of Natal, South Africa

RENCKEN, G. E. (1992). **Performance Studies of the Tubular Filter Press,** Ph.D. Thesis, Department of Chemical Engineering, University of Natal, South Africa

RICHARDSON, J. F. and ZAKI, W. N. (1954). **Sedimentation and Fluidisation : Part I,** *Transactions. Institute of Chemical Engineers.* 32(1), pp. 35-53

ROWE, P. W. and BORDEN, L. (1966). **A New Consolidation Cell,** *Geotechnique*, 16(2), pp. 162-170

SHIRATO, M. and ARAGAKI, T. (1966). **The Relationship Between Hydraulic and Compressive Pressures in Non-unidimensional Filter Cakes,** *Kagaku Kogaku*, 33(2), pp. 205-207

SHIRATO, M. and KOBAYASHI, K. (1967). **Studies in Non-unidimensional Filtration : Filtration on Cylindrical, Spherical and Square Surfaces,** Memoirs of the Faculty of Engineering, Nagoya University, 19(2), pp. 280-292

SHIRATO, M., KOBAYASHI, K. and TANIMURA, M. (1973). **Analysis of Constant Pressure Filtration of Compressible Cakes on Cylindrical Surface,** *Kagaku Kogaku*, 37(1), pp. 76-82

SHIRATO, M., MURASE, T., HIRATE, H. and MUIRA, M. (1966). **Studies in Non-unidimensional Filtration, Definition of Effective Filtration Area,** *Kagaku Kogaku*, 4(1), pp. 194-198

SHIRATO, M., MURASE, T., IRITANI, E. and HAYASHI, N. (1983). **Cake Filtration - A Technique for Evaluating Compression-Permeability Data at Low Compressive Pressure,** *Filtration and Separation*, September/October, pp. 404-406

SHIRATO, M., MURASE, T. and KOBAYASHI, K. (1968). **The Method of Calculation for Non-unidimensional Filtration,** *Filtration and Separation*, May/June, pp. 219-224

SHIRATO, M., SAMBUICHI, M., KATO, H. and ARAGAKI, T. (1969). **Internal Flow Mechanisms in Filter Cakes,** *Journal of the American Institute of Chemical Engineers*, **15**(3), pp. 405-409

TILLER, F. M. and COOPER, H. (1962). **The Role of Porosity in Filtration Part V : Porosity Variation in Filter Cakes,** *Journal of the American Institute of Chemical Engineers*, **8**(4), pp. 445-449

TILLER, F. M. and GREEN, T. C. (1973). **The Role of Porosity in Filtration Part IX : Skin Effects with Highly Compressible Materials,** *Journal of the Americal Institute of Chemical Engineers*, **19**(6), pp. 1266-1269

TILLER, F. M. and LEU, W. F. (1980). **Basic Data Fitting in Filtration,** *Journal of the Chinese Institute of Chemical Engineers*, **11**, pp. 61-70

TILLER, F. M. and LU, W. M. (1972). **The Role of Porosity in Filtration Part VIII : Cake Nonuniformity in Compression-Permeability Cells,** *Journal of the Americal Institute of Chemical Engineers*, **18**(3), pp. 569-572

TILLER, F. M. and YEH, C. S. (1985). **The Role of Porosity in Filtration Part X : Deposition of Compressible Cakes on External Radial Surfaces,** *Journal of the American Institute of Chemical Engineers*, **31**(8), pp. 1241-1248

TILLER, F. M., YEH, C. S., CHEN, W. and TSAI, C. D. (1968). **Generalised Approach to Mathematical Solution of Solid-Liquid Separation Problems,** Proceedings World Congress III of Chemical Engineering, Tokyo, Volume 3, pp. 126-129